PHYSICAL REVIEW B VOLUME 36, NUMBER 1 1 JULY 1987

Domain-wall interactions. I. General features and phase diagrams for spatially modulated phases

Michael E. Fisher
Baker Laboratory, Cornell University, Ithaca, New York 14853

Anthony M. Szpilka*
General Electric Company, Corporate Research and Development, P.O. Box 8, Schenectady, New York 12301
(Received 1 December 1986)

A general formalism is developed for analyzing physical systems exhibiting uniaxial, spatially modulated, high-order commensurate phases which can be regarded as composed of homogeneous domains separated by "smooth," parallel domain walls. Experimental evidence for a variety of such phases is mentioned; they arise also in various discrete-variable models in $d>2$ spatial dimensions. The free energy may be exactly decomposed into a computationally useful form as a sum of domain-wall tensions, Σ, plus pair, triplet, and higher-order wall-wall interaction potentials $W_n(\{l_i\})$, which depend on the wall separations l_i, and on temperature, etc. The principal transitions between high-order modulated phases are determined by Σ and the nearest-neighbor pair interaction, $W_2(l)$, alone: only *simple periodic* phases, having a uniform interwall separation, are stabilized by $W_2(l)$; more complicated *mixed* phases, in which the wall separations alternate between two values in a regular pattern, are a consequence of *further-neighbor* or, in general, *many-wall* interactions which also determine the interfacial tensions between coexisting modulated phases. The general form of the $W_n(\{l_i\})$ at low temperature is elucidated and their explicit calculation by a transfer-matrix method for models with short-range couplings is outlined. A *quasitricritical* point, governed by the changing form of the wall pair interaction, is analyzed in detail.

I. INTRODUCTION

In the last few decades, increasingly many examples of complex periodic ordering have been discovered among materials with simple chemical compositions. In some cases, the overall structure can most easily be described as a set of homogeneous, simply ordered *domains,* broken at regular but comparatively long intervals by the appearance of well-defined localized *walls,* to give rise to a "high-order commensurate (C) phase." In the simplest cases, one may consider a "uniaxial" or "striped" phase, where this spatial modulation, say, of wavelength Λ, is assumed to occur in *one direction only,* the ordering along the orthogonal directions being simple and uniform. The phase in question may then be described as an $\langle A^k B \rangle$ phase, for example, where the stacking of k layers of character A composes a domain while the B layers represent walls; if the layer thicknesses are a and b, one has $\Lambda = ka + b$: see, e.g., Fig. 1. Another class of ordering arises in substances possessing *two* intrinsic periodicities which are relatively irrational or *incommensurate* (IC) with respect to each other. These two classes of complex ordering, high-order C and IC phases, may actually be quite similar in appearance. A two-dimensional adsorbed layer, for example, may exist in an IC phase if adsorbate and substrate periodicities are incommensurate. Adsorbate-substrate interactions will, however, often induce the lattice constant of the layer to lock in phase with that of the substrate over comparatively long distances, broken by "phase slips" or "discommensurations," which may be regarded as the "walls" separating adjacent "domains" of simple commensurate ordering. The distinction between a high-order C and an IC phase then depends merely upon whether the mean interwall spacing is rational or not.

In this paper, we present a general formalism for discussing such systems and, in particular, for analyzing statistical-mechanical models exhibiting commensurate uniaxial or striped phases. Section II provides an overview of the wide variety of physical systems with this type of ordering, which may be candidates for modeling within the framework expounded here. In the latter part of Sec. II, we also indicate the appropriate context for our work relative to existing explanations of striped phases.

The starting point of our formalism, set out in Sec. III, will be a decomposition of the *exact* free-energy density of a system as a sum of wall or surface tensions, $\Sigma(T,\mu,\ldots) \equiv W_1(T,\mu,\ldots)$, associated with individual domain walls, plus wall-wall interaction potentials to account for the effective forces exerted by the walls on each other. For the decomposition to be exact, it is necessary, in general, to include n-wall interaction potentials, $W_n(T,\mu,\ldots;l_1,l_2,\ldots,l_{n-1})$, for *all* $n \geq 2$. Here W_n accounts for the incremental free energy, at some fixed values of temperature T, chemical potential μ, and other thermodynamic variables, of a configuration of n walls at successive separations $l_1,l_2,\ldots,l_{n-1}$, over and above the contributions to the free energy of "nearest-neighbor" j-wall interactions W_j for all $1 \leq j < n$. Thus, W_2 is just a "pair potential" acting between nearest-neighbor pairs of walls, W_3 is a "three-body potential," and so on.

The main features of the phase diagram are then governed simply by the behavior of the tension, $\Sigma \equiv W_1$, and the two-wall interaction, W_2, as explained in Sec. IV.

In particular, we focus on the C-IC *transition* between the homogeneous, single-domain "C" phase devoid of walls, and the uniaxial, striped or "IC" phase. Here the designation "IC phase" is intended to include both high-order C and truly IC phases: our analysis concentrates on low temperatures, where it turns out that these striped "IC phases" are in fact high-order C phases. The primary C-IC transition occurs near the locus of vanishing surface tension, $\Sigma(T,\mu,\ldots)=0$, and can be either *quasicontinuous* or *first order,* depending on whether $W_2(l)$ remains positive while decaying to zero, or exhibits a negative minimum. In Sec. V, we examine the role of the higher-order interactions $W_{n\,(\geq 3)}$ in further refining the phase diagram by stabilizing *or* excluding more complicated "mixed" phases like $\langle A^k B A^{k'} B \rangle$ $(k \neq k')$, etc.

For systems with *short-range* couplings, the general nature of the $W_n(\{l_i\})$ can be anticipated. Furthermore, for models with couplings of strictly finite range, expressions for the W_n which are asymptotically exact at low temperatures may be calculated by a *transfer-matrix* method, whose general features we outline in Sec. VI. Within the context of the matrix formalism, we analyze, in Sec. VII, a hitherto uninvestigated *quasitricritical point* which can appear on the phase diagram when, as a function of temperature or other thermodynamic variables, the functional form of $W_2(l)$ switches between the behaviors characterizing first-order and quasicontinuous C-IC transitions. We have carried out transfer-matrix calculations of the W_n for two specific models, the three-state chiral clock model[1-4] and the axial next-nearest-neighbor Ising (ANNNI) model:[5-8] details and the results, which reveal new and unexpected features of the phase diagrams of these models, will be presented in Parts II and III.[9] A brief account summarizing both this paper and those results has been published.[10]

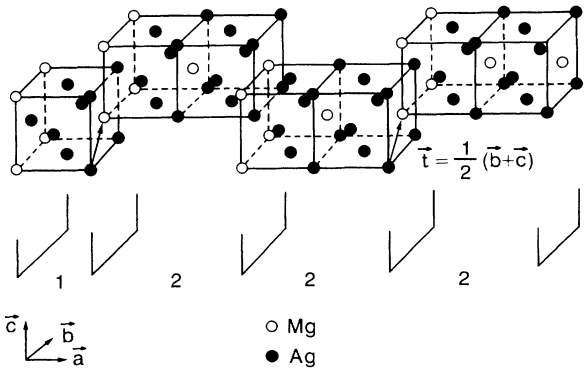

FIG. 1. The $\langle 12^3 \rangle$ structural phase of Ag_3Mg, after Portier *et al.* (Ref. 19). The structure is composed of two types of (**b**,**c**) planes, which alternate along the *a* axis: each type of plane contains a square array of Ag ions (filled circles); at the center of each square is either a Mg ion (open circle) or another Ag ion. There are thus Mg ions only in every other plane. [Only a fraction of each (**b**,**c**) plane is shown for clarity.] Adjacent planes are displaced by $\frac{1}{2}\mathbf{b}$ relative to each other; an additional relative displacement of $\mathbf{t}=\frac{1}{2}(\mathbf{b}+\mathbf{c})$ marks the end of each 2- or 1-band.

II. SYSTEMS WITH UNIAXIAL MODULATED PHASES

Recent reviews of the experimental situation have been provided by Bak,[11] by Pokrovsky and Talapov,[12] and, for three-dimensional systems, by Currat.[13] A short but informative review of three specific systems is given by Axe.[14] Our aim here is to highlight a few features of relevance to our analysis, to introduce notation, and to set the general background briefly.

A particularly interesting system exhibiting high-order magnetically ordered C phases is the rare-earth alloy CeSb, studied by Rossat-Mignod *et al.*[15] The highly anisotropic Ce-Ce exchange causes the $\langle 100 \rangle$ directions to be the easy spin axes.[16] Thus at low temperatures, all the Ce moments in each plane normal to a [100] axis are aligned predominantly parallel (↑) or antiparallel (↓) to [100]. In zero field at low T, these planes are stacked in a regular "two-up, two-down" sequence, $\cdots\uparrow\uparrow\downarrow\downarrow\uparrow\uparrow\downarrow\downarrow\cdots$, conveniently denoted $\langle 2\bar{2} \rangle$, or more simply, just $\langle 2 \rangle$.[5,17] If an external field $\mathbf{H}\|[100]$ is now applied, the $\langle 2 \rangle$ ordering undergoes a series of transitions to phases in which the sequence of "2-bands" (i.e., pairs of planes with parallel magnetizations) is interrupted at regular intervals by "1-bands" (i.e., oppositely magnetized *single* layers): experiments have (so far) revealed $\langle \bar{1}2\bar{2}2 \rangle \equiv \langle 12^3 \rangle$ (with periodic sequence $\downarrow\uparrow\uparrow\downarrow\uparrow\uparrow$), and $\langle 12 \rangle$ $(\cdots\downarrow\uparrow\uparrow\cdots)$, before a purely ferromagnetic phase, $(\cdots\uparrow\uparrow\uparrow\uparrow\cdots)$ or $\langle \infty \rangle$, sets in at large fields. In the $\langle 12^k \rangle$ phases, the 1-bands can evidently be considered as "walls" separating $\langle 2 \rangle$ domains of width k 2-bands; the pure $\langle 2 \rangle$ phase then corresponds to $k \to \infty$. It is plausible that experiments which scan the $\langle 2 \rangle$ phase boundary more closely will discover further interpolating phases with odd $k \geq 5$. At higher temperatures in zero field the experiments show planes with zero mean magnetic moment which, together with two oppositely magnetized adjacent planes, form a new type of wall which we may, for brevity, denote $\tilde{3}$. (A more systematic but clumsier notation would be $\bar{1}\,\mathring{1}\,1$.) As T falls below T_N, the highest zero-field transition point, the sequence of phases $\langle 2^k\tilde{3} \rangle$ with $k=0,1,2,3,4,5$ (and ∞) is seen.[15]

Once a particular type of wall and underlying phase, 1 or $\tilde{3}$ and $\langle 2 \rangle$ in CeSb, are identified, the simple periodic phases like $\langle 12^k \rangle$ and $\langle 2^k\tilde{3} \rangle$ might be denoted simply as $[l]$, where l $(=2k+1$ or $2k+3$ for the CeSb phases) represents the separation of successive walls measured, say, in units of a lattice spacing, a. This is the convention we will adopt in presenting the general theory below.

The analogs of the $\langle 12^k \rangle$ magnetic phases of CeSb have been seen also in various *structurally* characterized phases of binary alloys: see the review by de Fontaine and Kulik.[18] The ordered bands can be observed directly via high-resolution electron microscopy. Thus Portier *et al.*[19] report that the equilibrium structure of Ag_3Mg is the $\langle 12^3 \rangle$ phase illustrated in Fig. 1; as the Mg content of this alloy is varied from 26.5 at. % to 22 at. %, however, the structures $\langle 12^k \rangle$ for $k=2,3,4,6$, and, finally, ∞ (i.e., the pure $\langle 2 \rangle$ phase) arise successively. The more complicated "mixed phase" $\langle 12^3 12^4 \rangle$ was also seen. If we focus just on the wall spacings, this alternating structure may

(and will) be denoted $[l,l']=[2k+1, 2k'+1]=[7,9]$.

Similarly, van Tendeloo and Amelinckx[20] find periodic phases $\langle 2^k 3\rangle$, with $k=0$, 3, 4, and ∞, in Au_4Zn, and Loiseau *et al.*[21] report over a dozen phases composed of 1- and 2-bands in $Ti_{1+x}Al_{3-x}$, including higher-order mixed phases like $\langle 12(122)^2\rangle$, which we will denote as $[l,l',l'']=[3,5,5]$. Loiseau *et al.*[21] point out that the fundamental periods of all the phases which they observed can be derived from $\langle 1\rangle$ and $\langle 2\rangle$ by a branching process: e.g., $\langle 1\rangle$ combines with $\langle 2\rangle$ to yield $\langle 12\rangle$; then $\langle 1\rangle$ with $\langle 12\rangle$ yields $\langle 112\rangle$, and $\langle 12\rangle$ with $\langle 2\rangle$ yields $\langle 122\rangle$; then $\langle 122\rangle$ with $\langle 2\rangle$ yields $\langle 12^3\rangle$, etc. All these combinations are among the observed phases. A similar "branched" sequence of intermediate phases has been detected by Komura and Kitano[22] at the hcp-to-fcc transition of various Mg-based Friauf-Laves ternary alloys like $Mg(Cu_{1-x}Zn_x)_2$. One of our theoretical aims here is to understand this branching process, the extent to which it proceeds, and the resulting phase diagrams on a more general microscopic basis.

The physical mechanisms responsible for the appearance of these high-order phases in binary alloys are still debated. The oldest explanations proposed note that a periodic structural modulation will be stabilized in an electron-band picture if it introduces new Brillouin-zone boundaries close to flat portions of the alloy's Fermi surface.[18] (This explanation is also invoked to account for the stability of charge-density waves in transition-metal dichalcogenides.) Insofar as it is based on the minimization of electronic energy, however, the argument should be most directly applicable at low temperatures; yet the high-order C phases of binary alloys often disappear as the temperature is lowered. This suggests[18] that entropic or fluctuation effects, which require description by statistical-mechanical models, play a significant role. In particular, owing to independent theoretical progress,[5–8] attention has focused[23] on the so-called axial next-nearest-neighbor Ising (ANNNI) model, an Ising model with competing first- and second-neighbor ferromagnetic and antiferromagnetic couplings. In a subsequent paper[9] we shall describe the analysis of the ANNNI model according to the methods presented here.

More recently, Bruinsma and Zangwill[24] have modeled the periodic phases in the Mg-based ternary alloys[22] by a three-state Potts model with long-range forces: they used only energy minimization and found it necessary to supplement the model with terms describing elastic lattice distortions in order to obtain the experimentally observed higher-order "mixed" phases. They neglect all thermal fluctuation and entropic effects, arguing that such stabilization mechanisms are "ruled out since high-resolution electron-microscope lattice images show that the stacking-fault boundaries (which are the corresponding domain walls) of long-period close-packed structures are quite flat." This is an inadequate argument, however: the observations cited merely mean that the walls are statistically "smooth" as against statistically "rough." In a three-dimensional system one expects walls, surfaces, and interfaces of all sorts to be smooth and well localized in crystalline systems *below* a roughening temperature, T_R, but to undergo a transition to a "rough" or "diffuse" phase above T_R: the stability of *both* wall phases at nonzero T is determined by thermal fluctuations.[25,26] In fact, the long-period domain walls in the ANNNI model at low T are perfectly smooth and well localized even though the many distinct phases are stabilized entirely by thermal fluctuations.[5,8] In the case of the $Ag_{3-x}Mg_{1+x}$ alloys, both the 1-band walls and the 2-bands in the domains are seen to be straight and sharply delineated.[19] However, in some alloys, like AuCu II, striped phases are found in which the domain walls do appear diffuse or "wavy."[27] It is possible that some new mechanism is at work, but it seems plausible that one is simply seeing instances in which originally smooth, flat domain walls have undergone a roughening transition as the temperature is raised.[23,25] In the latter case, an intrinsically statistical-mechanical treatment is certainly called for.

High-order C structures or "polytypes" are also found in many minerals;[28,29] for example, $\langle 1\rangle$, $\langle 2\rangle$, $\langle 3\rangle$, and $\langle 13\rangle$ phases have been seen in Ni_2SiO_4-$NiAl_2O_4$: under applied pressure, $\langle 2\rangle$ transforms to $\langle 122\rangle$ and then to $\langle 12\rangle$.[28] It is not certain that all the observed structures are equilibrium phases, but reversible transitions such as $\langle 1\rangle \rightleftarrows \langle \infty\rangle \rightleftarrows \langle 3\rangle \rightleftarrows \langle 2\rangle$ have been observed in SiC.[29] Moreover, it is worth stressing that existing theories which predicate the growth of these structures from screw dislocations or stacking faults either predict types of disorder in the crystals which are seldom seen, or yield small energy differences among the various structures.[29] By contrast, Yeomans and Price[30] have had appreciable success in reproducing some observed polytype sequences on the basis of the low-temperature phase diagram of an ANNNI model extended to include third-neighbor axial spin-spin couplings.

Apparently true incommensurate (IC) phases in $(d=3)$-dimensional systems are seen in ferroelectrics. Thus in deuterated thiourea, $SC(ND_2)_2$, the modulation wave vector, $q(T)$, varies smoothly with T but then locks in at $qa=1/9$ (a being the lattice parameter) at $T\leq 193$ K.[31] Imposition of applied electric fields (up to 1800 V/mm), however, led to the observation by Moudden, Moncton, and Axe,[32] of commensurate $\langle 7^k 8\rangle$ phases, with $qa=(k+1)/(7k+8)$, for $k=1$, 3, and 5. (However, their findings have been disputed by Durand *et al.*,[33] who saw no such phases.) Yamada and Hamaya[34] have discussed similar C phases within ferroelectrics of composition A_2BX_4 on the basis of an ANNNI model with axial third-neighbor couplings.

Insight into the question of domain walls in IC phases is provided by the work of Blinc *et al.*[35,36] on Rb_2ZnCl_4. From the inhomogeneous broadening of NMR line shapes, they concluded that the "volume density of solitons (domain walls)," i.e., the ratio of wall width to interwall spacing within the IC regime, rapidly decreased from unity as T was lowered through the paraelectric-IC critical point. This supports the picture of an IC phase below criticality as a set of C domains separated by fairly well-defined walls, in contrast to the near-critical phase with a smooth, quasisinusoidally varying order parameter. The interwall spacing was seen to diverge[36] on approach to the low-temperature transition to the C phase. However, a domain-wall structure and the locking in of C phases

are not universal features of IC phases in ferroelectrics.[37]

Staged graphite intercalates provide another example of equilibrium uniaxial high-order C phases. Here, in stage n, there are n graphite layers between every successive pair of intercalate layers, which can be regarded as the "walls." Beyond these "simple" staged structures, which have been observed[38] up to $n=10$, one can contemplate mixed staging patterns with, e.g., alternating spacings: some recent evidence for such patterns has arisen both from theory and experiment.[39–41] It is also possible for a given stage-n intercalate, with n fixed, to exhibit various phases characterized by different stacking sequences of the intercalate layers themselves. In stage-2 graphite-Cs, for example, Winokur and Clarke[42] have observed that the stacking of the Cs layers, which evolves from fcc to hcp upon heating, exhibits at least two of the intermediate phases seen in the Mg-based Friauf-Laves ternary alloys mentioned above. Here, again, a wall-domain picture should apply.

The simplest microscopic approach to spatially modulated phases is provided by the $(d=1)$-dimensional Frenkel-Kontorowa model[11] of particles joined to nearest neighbors by harmonic springs of natural length b_0, but subject also to a sinusoidal "substrate" potential of period a_0 and amplitude V. When the mean interparticle spacing is near that for a C phase of *order* p, one defines the "natural misfit" by

$$\delta \equiv 2\pi(b_0 - pa_0)/pa_0 \ . \tag{2.1}$$

The ground-state properties of the continuum version of this model were obtained by Frank and van der Merwe.[43] A general configuration consists of domains, in which the particles are in close registry with the substrate potential, separated by relatively short misfit regions which constitute the domain walls (or "solitons"). The mean interwall spacing l adjusts itself to yield the appropriate mean linear density of particles set by b_0. As b_0 and hence δ vary, a C-IC transition occurs in the ground state. Near this transition, when the walls are widely spaced so that the incommensurability $\Delta q \propto 1/l$ is small, the energy per unit length of the system assumes the form[44,11]

$$E(\Delta q;\delta) = (8\sqrt{V} - 2\pi\delta)\Delta q + 32\sqrt{V}\,\Delta q\, e^{-\sqrt{V}/\Delta q} \ . \tag{2.2}$$

Now one may interpret the coefficient of Δq as an energy or "tension" per wall: the second term then represents an exponentially decaying *wall-wall repulsion.* This interpretation, in fact, forms the central theme of our analysis: the exact energy (or free energy) can be expressed as a sum of terms associated with individual walls, plus terms which decay as the interwall separation $l \propto 1/\Delta q$ increases. Note that for

$$\delta < \delta_c \equiv 4\sqrt{V}/\pi \ , \tag{2.3}$$

the energy density (2.2) is minimized by taking $\Delta q \equiv 0$, which corresponds to the ideal commensurate phase of order p. On the other hand, when $\delta > \delta_c$, the first term of (2.2) is negative for $\Delta q > 0$, corresponding to a *negative* and, hence, intrinsically unstable tension. The energy E is then minimized by some nonzero value of Δq, corresponding to a finite spacing, l, of the walls. Thus an IC phase is stabilized by the wall-wall repulsions embodied in the second term. In particular, minimizing (2.2) shows that the incommensurability vanishes *logarithmically* near the C-IC transition according to

$$\Delta q \propto 1/l \sim 1/\ln(\delta - \delta_c)^{-1} \ . \tag{2.4}$$

A more realistic treatment of uniaxially modulated phases must allow for destabilizing fluctuations at nonzero T and for stabilizing interactions in transverse dimensions. A semimicroscopic theory of uniaxial C-IC transitions in arbitrary spatial dimensions d has been advanced.[45,46] The key ingredients of the free-energy density in this theory are: (i) the surface tension of an isolated wall, which vanishes linearly on approach to the transition as in the first term of (2.2); (ii) an exponential wall-wall repulsion as in the second term of (2.2), with a length scale set by the bulk correlation length, $\xi_\infty(T,\mu,\ldots)$, within a single domain; and (iii) entropic terms arising from large-scale fluctuations in the locations of the walls, modified by the restriction that walls may not touch or cross. This last feature presupposes *rough* delocalized walls, i.e., $T > T_R$. Minimization of the resultant free energy to find the incommensurability yields[45]

$$\Delta q \propto 1/l \sim (\delta - \delta_c)^{\bar{\beta}} \tag{2.5}$$

with

$$\bar{\beta}(d) = \frac{3-d}{2(d-1)} \quad \text{for } 1 < d \le 3 \ ,$$
$$= 0 \quad \text{for } d \ge 3 \ , \tag{2.6}$$

there being no C-IC transition at nonzero temperatures when $d=1$. The value $\bar{\beta}=0$ for $d \ge 3$ indicates a return to the logarithmic vanishing of Δq as in (2.4): evidently, $d=3$ is the upper critical dimension for the relevance of long-wavelength fluctuations in the walls. These large-scale fluctuations, in fact, generate an effective wall-wall repulsion with a potential energy[45–48]

$$W(l) \propto \frac{k_B T}{l^\tau} \quad \text{with } \tau = \frac{2(d-1)}{3-d} \ , \tag{2.7}$$

for $d < 3$. This slow power-law decay is what leads to the behavior (2.5).

The value $\bar{\beta}(d=2)=\frac{1}{2}$ agrees with the result obtained by Pokrovsky and Talapov[49] from an exact solution of a version of the Frank–van der Merwe Hamiltonian in $d=2$ dimensions in which the walls may not cross or mutually annihilate. In real two-dimensional systems, however, p adjacent domain walls can and, statistically, will touch and annihilate one another in point dislocations (or "vortices"). One effect of these dislocations is to render a continuous C-IC transition boundary unstable to an intermediate disordered phase when the order p of the C domains is too small.[50,51] At higher temperatures they lead to a Kosterlitz-Thouless transition. In the present work, however, we shall concentrate on $d > 2$ dimensions, and can therefore ignore dislocations since, as line defects, their large free energy strongly suppresses their equilibrium density. Likewise, for $T < T_R$ or for $d > 3$ the walls

will be smooth, and long-wavelength fluctuations, leading to power laws like (2.7), will not play a dominant role. Rather the issue will be to understand the more detailed behavior of the wall-wall interactions as mediated by fluctuations of finite spatial range and their effects on the phase diagram.

Finally, one must note that direct long-range forces of van der Waals character, electrostatically generated, etc., may play a role. Random impurities of various sorts can also modify the nature of the C-IC transition, changing the value of the exponents τ and $\bar{\beta}$, or can even destroy the transition.[52–56]

III. WALL INTERACTIONS: DEFINITIONS AND GENERAL CHARACTER

Our aim now is to develop a systematic treatment of systems which, under appropriate conditions of temperature, T, chemical potential, μ, or other thermodynamic fields, exhibit uniaxial, spatially modulated phases which can be viewed as consisting of homogeneous domains of some underlying ordered commensurate phase, C, separated by parallel domain walls. In the simplest situation, each domain wall will be physically equivalent to all the others: this implies that the underlying C phase is characterized by some p-fold discrete symmetry ($p=2,3,\ldots$) which we may suppose is just Z_p, i.e., cyclic. We will confine ourselves to this situation although some of our considerations apply in the absence of domain symmetry or can be readily modified to allow for other symmetries.

For concreteness, suppose the system has a lattice structure of $N=L_\perp^{d-1}L$ sites where L is the length of the system in the relevant axial direction measured in lattice spacings while, in d dimensions, $L_\perp$ represents the corresponding cross-sectional width. Let $\mathcal{F}_N(T,\mu,\ldots)$ denote the total free energy of the system which, in general, will have a dependence on the details of the boundary conditions which we will specify as appropriate.

Consider now a region of the phase diagram, i.e., $(T,\mu,\ldots)$ space, in which C is the stable bulk phase. Two coexisting domains of "adjacent" symmetry character will be separated by an interface or domain wall which will have a "tension," i.e., free energy per unit area, $\Sigma(T,\mu,\ldots)$. The presence of a domain wall normal to the axial direction can be ensured by imposing appropriate boundary conditions on the perimeters of the $L_\perp^{d-1}$ cross sections which serve to specify the character of the contiguous domain. This is illustrated in Fig. 2(a) for an Ising-like or $p=2$ system in which the two distinct phases are selected by $+$ or $-$ ordering fields on the boundary. Note that the boundary conditions specify both the mean location *and* mean orientation of the wall. The tension of the wall will be independent of its location but *will* in general depend on its orientation. Since we are interested in equilibrium, i.e., minimal-free-energy phases containing domain walls, we suppose the axial direction is specified so that the tension is minimal for the corresponding wall orientation. Now let

$$F_0(T,\mu,\ldots)\equiv\mathcal{F}_N^{(0)}(T,\mu,\ldots)/N$$

denote the free energy per site of the system with no walls and, say, with all $+$ boundary conditions, while $F_1(T,\mu,\ldots)\equiv\mathcal{F}_N^{(1)}/N$ is the corresponding free energy with one wall specified by the $(+,-)$ boundary conditions of Fig. 2(a). Then the tension or single-wall potential, W_1, is given by the excess free energy $(\mathcal{F}_N^{(1)}-\mathcal{F}_N^{(0)})/L_\perp^{d-1}$ or, more precisely, by

$$\Sigma(T,\mu,\ldots)\equiv W_1(T,\mu,\ldots)=\lim_{L\to\infty}L[F_1(T,\ldots)-F_0(T,\ldots)]\,, \quad (3.1)$$

where the limit $L_\perp\to\infty$ is also understood. Note that this definition is perfectly satisfactory whether the wall is "smooth," and hence "flat" as it will be for T less than the roughening temperature T_R, or whether it is "rough" and hence "wanders" in a diffuse manner as above T_R.

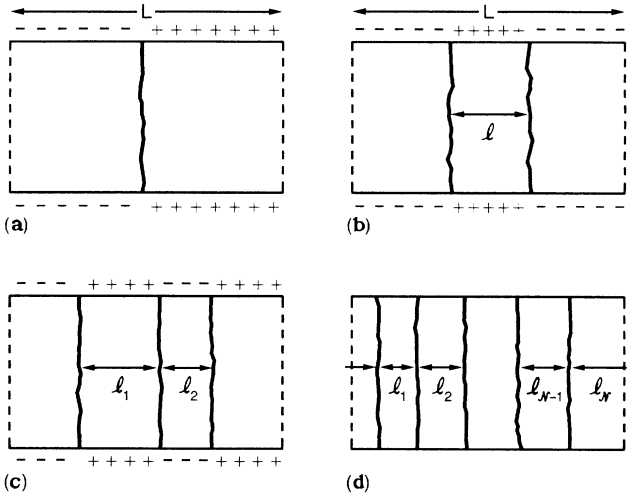

FIG. 2. (a) Schematic cross section of a lattice system exhibiting two homogeneous domains separated by a domain wall stabilized in mean position and orientation by ordering fields, denoted $+$ and $-$ (as appropriate for an Ising-like system), imposed on the boundaries. The length of the lattice in the axial direction, normal to the walls, is L. (b) and (c) Corresponding configurations with two domain walls at separation l, and three walls at separations l_1 and l_2, respectively. (d) A general configuration of $\mathcal{N}$ walls at successive spacings l_i $(i=1,2,\ldots,\mathcal{N})$, as might represent a spatially modulated phase; periodic boundary conditions have been assumed.

A. Domain-wall interactions

Now consider the two-wall configuration enforced by the boundary conditions illustrated (for $p=2$) in Fig. 2(b). We can associate to each wall its tension, Σ, but the total free energy $\mathcal{F}_N^{(2)}\equiv NF_2(T,\mu,\ldots;l)$ for the two walls at separation l will, in general, differ from the sum $\mathcal{F}_N^{(0)}+2\Sigma L_\perp^{d-1}$. This difference can be ascribed to *wall-wall interactions* with a potential (free) energy per unit area

$$W_2(T,\mu,\ldots;l)=\lim_{L\to\infty}L[F_2(T,\ldots;l)-F_0(T,\ldots)]-2\Sigma(T,\ldots)\,. \quad (3.2)$$

Formally, this definition of the wall pair interaction is quite satisfactory but some cautionary words are needed.

If the walls are *rough* their mean positions need no longer be those specified by the boundary conditions; likewise l may *not* correctly represent the mean wall separation. The reason is simply that a rough wall can readily distort to lower the total free energy: thus, if the potential is repulsive the walls will, for large $L_\perp$, tend to bow outwards and move apart so that the mean separation exceeds l (and, in general, diverges[25,47] as $L_\perp \to \infty$). A more elaborate definition of $W_2(l)$ is then needed. This problem does not arise for smooth walls (with $T < T_R$), which is one reason many of our considerations will be essentially restricted to smooth walls for which the mean positions *remain "pinned" at definite locations* within the lattice. (Even for smooth walls, however, some caution is required to exclude *other* configurations of domain walls which may satisfy the same boundary conditions: to avoid such problems resort may be had to stabilizing bulk ordering fields which are allowed to vanish in an appropriate fashion as $L_\perp \to \infty$.)

Clearly we may proceed to define a triplet wall potential, $W_3(l,l')$, in analogous fashion by using the boundary conditions illustrated in Fig. 2(c). Specifically, if $F_3(l_1,l_2)=\mathcal{F}_N^{(3)}(l_1,l_2)/N$ is the free energy per site for a configuration of three walls with separations l_1 and l_2, we take

$$W_3(l_1,l_2)=\lim_{L\to\infty} L[F_3(l_1,l_2)-F_0] - 3\Sigma - W_2(l_1)-W_2(l_2)\ . \tag{3.3}$$

Likewise, the quadruplet potential will be defined by

$$W_4(l_1,l_2,l_3)=\lim_{L\to\infty} L[F_4(l_1,l_2,l_3)-F_0] - 4\Sigma - W_2(l_1)-W_2(l_2) - W_2(l_3)-W_3(l_1,l_2)-W_3(l_2,l_3)\ , \tag{3.4}$$

in which l_1, l_2, and l_3 denote the successive separations of the four walls. The higher-order $W_n(T,\mu,\ldots;l_1,\ldots,l_{n-1})$ follow in the same manner. Note that our definition of $W_3(l_1,l_2)$ does *not* subtract off the second-neighbor two-wall interaction $W_2(l_1+l_2)$; similarly, in defining $W_4(l_1,l_2,l_3)$, none of $W_2(l_1+l_2)$, $W_2(l_2+l_3)$, $W_2(l_1+l_2+l_3)$, nor $W_3(l_1+l_2,l_3)$ or $W_3(l_1,l_2+l_3)$ are subtracted. This is purely a matter of convention: in defining *many-particle* interactions it is customary to subtract *all* possible lower-order interactions even in one dimension where linear ordering allows the alternative natural choice we have made here. However, our convention turns out to be physically the more satisfactory for systems in which the underlying interactions, which generate the wall potentials, are of short range or decay rapidly. This is demonstrated by our explicit calculations for the ANNNI model[9] which show, for example, that the three-wall interaction, $W_3(l_1,l_2)$, as defined here is much *smaller* in magnitude than the customary three-wall term [that we would denote as $W_3(l_1,l_2)-W_2(l_1+l_2)$].

In certain models or approximate treatments of a model it may transpire that the interactions between, say, M domain walls can be expressed purely in terms of a direct pair potential, $\Phi(l_{ij})$, where $l_{ij}=l_i+l_{i+1}+\cdots+l_{j-1}$ is the total separation between walls i and j (with $j>i$). In other cases[7] the effective pair potential operative between walls i and j actually depends on the number of intervening walls, $m=j-i-1$, and one has only a pseudopair potential, say, $\Phi_{m+2}(l_{ij})$. For a single pair of walls one clearly has $\Phi_2(l)\equiv\Phi(l)=W_2(l)$. However, it is not hard to establish the *general* identity

$$W_n(l_1,l_2,\ldots,l_{n-1})=\Phi_n(l_1+l_2+\cdots+l_{n-1})\ , \tag{3.5}$$

where for pure pair potentials the subscript on Φ may be dropped. Thus any simplifications resulting from pure pair or pseudopair interactions are easily accounted for within the more general formalism.

B. Free-energy decomposition

Now consider a system with many parallel domain walls in a configuration specified by the spacings $\{l_i\}$; for convenience one may take periodic boundary conditions in the axial direction as in Fig. 2(d) so that, for $\mathcal{N}$ walls, $l_{\mathcal{N}}$ represents the separation between the $\mathcal{N}$th and first walls around the lattice. The overall free energy per site may now, by reverting the definitions, be expressed exactly as

$$\mathcal{F}(T,\mu,\ldots;\{l_i\})=F_0(T,\mu,\ldots)+\Delta\mathcal{F}(T,\mu,\ldots;\{l_i\}) \tag{3.6}$$

where the excess free energy is

$$\Delta\mathcal{F}(\{l_i\})=\frac{1}{L}\sum_{i=1}^{\mathcal{N}}\left[\sum_{n=1}^{\mathcal{N}} W_n(T,\mu,\ldots;l_i,l_{i+1},\ldots,l_{i+n-2})\right] =\frac{\mathcal{N}}{L}\Sigma(T,\mu,\ldots)+\frac{1}{L}\sum_{i=1}^{\mathcal{N}}[W_2(l_i)+W_3(l_i,l_{i+1})+\cdots]\ ; \tag{3.7}$$

the use of $\mathcal{F}$ serves to stress the functional dependence on the configuration $\{l_i\}$.

This decomposition of the total free energy of a system with walls will be our basic theoretical tool in analyzing the existence or absence of various modulated phases and their location and extent in the phase diagram. As we have derived it, the formula applies to a situation in which the pure C phase is the only thermodynamically stable phase: the walls are present only because of imposed boundary conditions (or further auxiliary fields) and, consequently, $\Delta\mathcal{F}$ is always positive. If the boundary conditions are relaxed (and other auxiliary fields removed) the configuration specified by the $\{l_i\}$ will (at best) be metastable. If one then asks for the *minimizing configuration*

one must find that it corresponds to the *absence* of all walls! Then $\Delta\mathcal{F}=0$ and $\mathcal{F}$ becomes $F_0(T,\mu,\ldots)$, the true equilibrium free energy per site.

On the other hand, if, as $T,\mu,\ldots$ vary, the increment $\Delta\mathcal{F}$ should vanish for some configuration $\{l_i\}$ (in the absence of stabilizing boundary conditions, etc.) it must signal the limit of stability of the pure C phase. If one then supposes that $F_0(T,\mu,\ldots)$, $\Sigma(T,\mu,\ldots)$, $W_2(T,\mu,\ldots;l)$, $W_3(T,\mu,\ldots;l,l')$, etc. may be *smoothly continued* beyond this limit, one may argue that the configuration, say $\{l_i\}=\{l_{i(0)}\}$, actually minimizing $\Delta\mathcal{F}$, which now takes some negative value, corresponds to a *new physical phase* with domain walls present in full bulk equilibrium. The minimal free energy $\mathcal{F}(T,\mu,\ldots;\{l_{i(0)}\})$ is then the true bulk free energy per site $F(T,\mu,\ldots)$. Note, however, that in the new phase the tension, $\Sigma(T,\mu,\ldots)$, which is normally regarded as intrinsically positive may, and in many situations will, be *negative*: of course, repulsive components of the wall interactions will serve to limit the density of such negative-tension walls.

The approach sketched here represents the philosophy we will adopt even though it is hard to justify on any rigorous basis. It should be reliable provided the phase transitions that arise are *continuous, quasicontinuous,* or only *weakly first order.* The problem encountered here is the same that arises when the isotherm of a gas is imagined as continuing beyond its condensation point to describe a metastable phase or, more generally, whenever one locates a phase boundary by "equating the free energies of two phases:" in reality, there is only one stable thermodynamic phase at a general point of the phase diagram and always only one bulk free energy. Consequently, the approach may break down well within the modulated phase region of the phase diagram. Nonetheless, it can be expected to give correct results near a transition from a pure, commensurate "single-domain" phase into a corresponding modulated phase: furthermore, since the "single-domain" or C phase may itself have a modulated structure the limitations are less severe than at first appears.

One may also argue *conversely* from the observed presence of domain-wall modulated phases in real systems (as discussed in Sec. II) or their demonstrated existence in model systems,[3–12] that a decomposition of the free energy in terms of a background free energy, F_0, a wall tension, Σ, and wall interactions, $W_2, W_3, \ldots$ which all *vary smoothly* with T, μ, etc., will provide a proper description of the phase behavior. This viewpoint will be explored generally in this paper and tested by explicit calculations for the ANNNI and chiral clock models in subsequent papers.[9,10]

C. Decay of interactions

For the decomposition (3.7) of the free energy to be of practical utility two conditions must be met. First, and most obvious, is that some concrete information about the $W_n(l_1,\ldots,l_{n-1})$ must be available. By their construction, each W_n *decays to zero* as any one of its arguments, l_i, becomes large; but the form of the decay, the nature of the variation at finite l_i, and the interplay of the arguments for $n\geq 3$ would seem relevant. In subsequent papers,[9,10] explicit calculations of W_2, W_3, etc. will be presented for the general ANNNI and three-state chiral clock models. However, it transpires that the topology of a system's phase diagram is largely determined by quite *general* features of the W_n, without the need for detailed calculations. This is demonstrated in the next section.

The second, but related, prerequisite for the usefulness of (3.7) is that not *all* the infinitely many W_n be of comparable importance in determining the phase diagram. Fortunately, this condition will be fulfilled under fairly general conditions. To see this, consider systems with *short-range interactions* under conditions not too close to the intrinsic disordering or melting temperature of the C phase itself and, as already mentioned, in situations where the domain walls are not rough. The significant correlations in the C phase, which will be dominated by "counterdomain" fluctuations, will, by virtue of the finite-range interactions, *decay exponentially* with a characteristic bulk *correlation length,* $\xi_\infty(T,\mu,\ldots)$. In general the correlation decay will be anisotropic; accordingly we will take ξ_∞ to denote the correlation length for the axial direction, i.e., normal to the domain walls. At low temperatures ξ_∞ will become small; indeed, in many systems it can be estimated by

$$\xi_\infty(T)\approx R_0 k_B T/\Delta\epsilon \quad (T\to 0)\ , \tag{3.8}$$

where R_0 is the range of the interactions (in the axial direction) while $\Delta\epsilon$ is the energy of a local counterdomain fluctuation on the scale of R_0.

Now the correlations within a C domain can be viewed as measuring the response at distance l from some local disturbance or inhomogeneity: this response, and associated free-energy increments, must decay as

$$e^{-\Gamma l}=w^l \ \text{ with } w\equiv e^{-\Gamma} \text{ and } \Gamma=a/\xi_\infty\ , \tag{3.9}$$

where, as previously, we suppose that distances, l, are measured in units of the lattice spacing a. Evidently, a smooth (i.e., nonrough) domain wall represents a localized disturbance. The response caused by a second wall at a distance l must then be of order w^l. This observation yields the estimate

$$|\,W_2(T,\mu,\ldots;l)\,|\sim\Delta\epsilon\, w^l\ . \tag{3.10}$$

Note the modulus bars: the sign of $W_2(l)$ is *not* clear *a priori.* If $R_\perp$ and $a_\perp$ are the transverse range of interactions and lattice spacing, respectively, a further factor $(a_\perp/R_\perp)^{d-1}$ should be included on the right-hand side since W_2 is a free energy per unit area of lattice cross section; but we may assume this factor is of order unity.

The analogous arguments apply for the addition of a third wall provided one recalls that the definition, (3.3), of $W_3(l,l')$ entails the subtraction of the dominant contributions $W_2(l)\sim w^l$ and $W_2(l')\sim w^{l'}$: the remaining term must vanish as either l or l' becomes large and hence varies as $w^{l+l'}$. Extending the argument clearly yields the *fundamental decay property*

$$|\,W_n(l_1,l_2,\ldots,l_{n-1})\,|\sim\Delta\epsilon\, w^{l_1+l_2+\cdots+l_{n-1}}\ , \tag{3.11}$$

which, to recapitulate, should hold generally for $(d\geq 3)$-

dimensional systems with short-range forces provided T is not too large. Note that the basic factor $w \equiv e^{-\Gamma}$ is always less than unity and will become small at low temperatures: we will thus regard w as a small parameter and use it to specify successive orders of approximation. In particular, we will see that, starting with $\Sigma \equiv W_1$ and $W_2(l)$, one need invoke W_3 and the higher W_n in the free energy (3.7) only when necessary to resolve some "degeneracy," i.e., near cancellation of lower-order terms, and so further refine the phase diagram. This procedure is examined systematically in the following sections.

By examining the propagation of correlations within C domains in further detail it is possible to develop a significant refinement of the decay estimate (3.11). This entails a transfer-matrix (or linear operator) formulation of the axial propagation of correlation providing, in essence, an extension of the classic Ornstein-Zernike analysis. This approach is expounded generally in Sec. VI below and applied in Sec. VII to discuss quasitricritical points on the C-IC transition locus for long-period modulated phases. The matrix technique can be implemented as an explicit computational scheme at low temperatures in discrete-variable models as will be demonstrated for the ANNNI and chiral clock models in subsequent papers. All the general features of the W_n, etc., identified here are confirmed by the explicit calculations.

Finally, note that owing to the structure of the C phase and the nature of the domain walls the spacing, l, between domain walls will be restricted, in general, to some "comb" of integral values, namely,

$$l = p_1 k + p_0 \quad \text{with } k = 0, 1, 2, \ldots \tag{3.12}$$

rather than to arbitrary integers. Thus for the $\langle 2^k 3 \rangle$ phases described in Sec. II one has $p_1 = 2$ and $p_0 = 3$ and so on. For simplicity in the general analysis below we will ignore this minor complication and suppose, explicitly, that $p_1 \equiv 1$; but then mixed phases, such as $[l, l+1]$, and phase boundaries such as $[l]:[l+1]$ must be interpreted generally as $[l, l+p_1]$ and $[l]:[l+p_1] \equiv [p_1 k + p_0]:[p_1(k+1)+p_0]$, etc.

IV. PHASE DIAGRAM: MAIN FEATURES

We will now use the decomposition (3.7), with the assumption that $\Sigma(T,\mu)$, $W_2(T,\mu;l)$, etc. are smooth functions of T and μ, in order to study the phase diagram in the (T,μ) plane. For simplicity we neglect thermodynamic fields beyond T and μ but stress that μ could denote a pressure, an external magnetic field, etc. In models, μ may denote, for example, a competition parameter, such as $\kappa = |J_2|/J_1$ in the ANNNI model, where J_2 and J_1 represent second- and first-neighbor axial couplings;[5-8] or a chiral symmetry-breaking field as in the chiral clock models,[1-4] etc.

In leading approximation (3.7) reduces merely to

$$\Delta\mathcal{F}(\{l_i\}) \simeq \Delta\mathcal{F}_1 = (\mathcal{N}/L)\Sigma(T,\mu) \ . \tag{4.1}$$

If Σ is positive the equilibrium state is given by $\mathcal{N}=0$, i.e., the absence of all walls, in other words, the original C phase which we will call $[\infty]$. Suppose, however, that Σ vanishes and changes sign on a locus, $T = T_0(\mu)$, and is negative for, say, $T > T_0(\mu)$, as illustrated in Fig. 3. Then the stable phase for $T > T_0(\mu)$ corresponds, formally, to $\mathcal{N} = \mathcal{N}_{\max}$ which describes a strongly modulated, striped phase of close-packed domain walls with spacing $l_{(0)} = p_0$ [see (3.12)] which we will call $[p_0]$. If, as we suppose, Σ vanishes linearly as $T \to T_0$ according to

$$\Sigma(T,\mu) \approx \Sigma'(T)[T_0(\mu) - T] \equiv -\Sigma' \delta T(\mu) \ , \tag{4.2}$$

with, for concreteness, $\Sigma' > 0$, the phase transition will, clearly, be first order in character. In this circumstance, it may well be that the modulated phase differs so strongly from the original C phase that the domain walls no longer retain their original character and the postulated description breaks down; however, if the transition is not too strong the theory should remain approximately valid, the free energy of the modulated phase $[p_0]$ satisfying

$$F(T,\mu) \simeq F_0(T,\mu) - p_0^{-1} |\Sigma(T,\mu)| \ . \tag{4.3}$$

To improve this crude first-order picture one should, clearly, introduce the pair wall interactions which must play some role once the domain-wall spacing is not extremely large. In second order we may write

$$\Delta\mathcal{F} \simeq \Delta\mathcal{F}_2(\{l_i\}) = \frac{1}{L} \sum_{i=1}^{\mathcal{N}} l_i G(T,\mu;l_i) \tag{4.4}$$

with individual wall free energy per site

$$G(T,\mu;l) \equiv l^{-1}[\Sigma(T,\mu) + W_2(T,\mu;l)] \ . \tag{4.5}$$

If we accept the estimate (3.11), one sees that the domain-wall interactions should play a significant role in

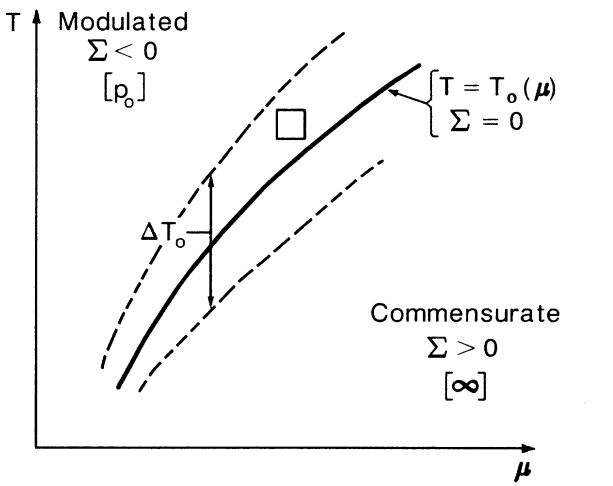

FIG. 3. Schematic phase diagram for a system of noninteracting walls, with the first-order free-energy density (4.1) determined solely by the surface tension $W_1 = \Sigma$, which vanishes on the locus $T = T_0(\mu)$. For $\Sigma > 0$, no walls are present; for $\Sigma < 0$, walls are spaced as closely as possible: the resulting phases are denoted $[\infty]$ and $[p_0]$, respectively. The dashed lines bound the transition region, of width $\Delta T_0(\mu)$ given by (4.6), within which the phase diagram may be altered by the inclusion of wall interactions, $W_2, W_3, \ldots$ in the free-energy expression. The small square to the left of the transition locus, $\Sigma = 0$, is magnified in Fig. 8 below (which shows a possible appearance of that region when W_2 is included).

a transition region around the locus $T_0(\mu)$ defined by

$$|\Sigma| \approx \Sigma' |T - T_0(\mu)| \lesssim \max_l |W_2(l)| \simeq W_2(p_0) \sim \Delta\epsilon\, w^{p_0} . \quad (4.6)$$

The width, ΔT_0, of the transition region is thus of order $W_2(T_0,\mu;p_0)/\Sigma'$.

Now the behavior within the transition region can be broadly categorized into two characteristic cases which we will analyze separately: (A) The pair potential, $W_2(l)$, remains *positive,* i.e., "totally repulsive," for all l ($\geq p_0$) although, by definition, decaying to zero as $l \to \infty$: see, e.g., Fig. 4; (B) the potential $W_2(l)$ has a unique, *negative* (i.e., "attractive") *absolute minimum* at some $l = l_{(M)} < \infty$: see, e.g., Fig. 6, below.

A. Case (A): Quasicontinuous C-IC transition; devil's last step

To find the set of wall spacings, $\{l_i\}$, minimizing $\Delta\mathcal{F}_2$ in (4.4) it is advantageous to consider, first, *simple periodic phases* in which $l_i = l$ is *constant* (all i): such phases will be denoted $[l]$. For these phases the free energy $\Delta\mathcal{F}_2$ becomes, for $L \to \infty$, simply equal to $G(T,\mu;l)$ in (4.5). Suppose the tension Σ is initially positive. Since $W_2(l) \geq 0$ for all l the minimum is attained for $l = l_{(0)} = \infty$ where $G(l)$ vanishes. Thus the C phase, $[\infty]$, remains stable for $T < T_0(\mu)$. Once Σ is negative, however, $G(l)$ must also be negative for sufficiently large l since $W_2(l) \to 0$. To find the minimizing spacing $l_{(0)}$, note that $G(l)$ can be regarded as the *slope,* on a plot of $W_2(l)$ *vs* l (see Fig. 4), of the line through the points (l, W_2) and $(0, -\Sigma)$. The required spacing, $l_{(0)}$, is just that value for which the slope is most negative; the implied graphical construction is illustrated in Fig. 4. Note that if l is regarded as a continuous variable then the line determining $l_{(0)}$ is a tangent to the plot of $W_2(l)$. Indeed if $W_2(l)$ is differentiable the minimization condition $G'(l_{(0)}) = 0$ can be rewritten simply as

$$W_2'(l_{(0)}) = [\Sigma + W_2(l_{(0)})]/l_{(0)} = G(l_{(0)}) . \quad (4.7)$$

Since $W_2(l) \to 0$ there is no upper bound to the value of $l_{(0)}$ as T and μ and, hence, Σ vary. In other words, as the phase boundary, $T_0(\mu)$, is approached from the modulated or "incommensurate" side, infinitely many periodic phases of increasing period, $l_{(j)}$, become stable. From the construction it is also clear that as $-\Sigma$ decreases, the values of $l_{(j)}$ *increase monotonically.* However, the jumps in $l_{(j)}$ need not consist of unit steps [or steps of size p_1: recall (3.12)]. This is illustrated in Fig. 4(b), where $l_{(j)}$ jumps from l^- to l^+ as $-\Sigma$ decreases through $-\Sigma_0$, which value thus represents a point of first-order phase transition. Apart from such successive points of transition, $G(l)$ always possesses a *unique* minimum at $l = l_{(0)}$. Note that, here and below, we implicitly neglect the variation of $W_2(T,\mu;l)$ with T and μ and focus only on the l-dependence: this simplification is valid for small $\exp(-\Gamma l_{(0)})$, as demonstrated in the Appendix.

If $W_2(l)$ is a *strictly convex* function, defined by the condition

$$\Delta^2 W_2(l) \equiv W_2(l+1) - 2W_2(l) + W_2(l-1) > 0 \quad (4.8)$$

or, if l is regarded as a continuous variable, by

$$d^2 W_2/dl^2 > 0 , \quad (4.9)$$

it is easy to see that *all* the successive phase transitions $[l] \to [l+1]$ will occur. Conversely, all consecutive spacings will appear as stable phases only if $W_2(l)$ is strictly convex. More generally the allowed values, $l_{(j)}$, in the sequence of periodic phases, $[l_{(j)}]$ ($j = 1,2,3,\ldots$), generated as Σ varies, will be all those for which $W_2(l)$ coincides with its *convex cover,* $\tilde{W}_2(l)$.[57]

We have spoken above as if the minimization of $G(l)$ were sufficient to minimize the full second-order free-energy functional, $\Delta\mathcal{F}_2(\{l_i\})$ in (4.4). To prove that this is, in fact, the case, note that since $L = \sum_{i=1}^{\mathcal{N}} l_i$, the requisite free-energy difference can be written

$$\Delta\mathcal{F}_2(\{l_i\}) - G(l_{(0)}) = \frac{1}{L} \sum_{i=1}^{\mathcal{N}} l_i [G(l_i) - G(l_{(0)})] . \quad (4.10)$$

But, provided Σ is not at a transition point of G, the value $l = l_{(0)}$ locates the unique minimum of $G(l)$. It follows that each bracketed term in the sum here must be nonnegative with equality achieved only if $l_i = l_{(0)}$. Consequently, under the approximation $\Delta\mathcal{F} \simeq \Delta\mathcal{F}_2$ of the system's free energy, *all stable phases are simple periodic phases. At* a point of transition, say from l^- to l^+, each l_i must, in order to minimize $\Delta\mathcal{F}_2$, take only the values l^- or l^+: to elucidate the optimal configuration more precisely requires a study of $W_3(l,l')$, etc., which is undertaken in Sec. V.

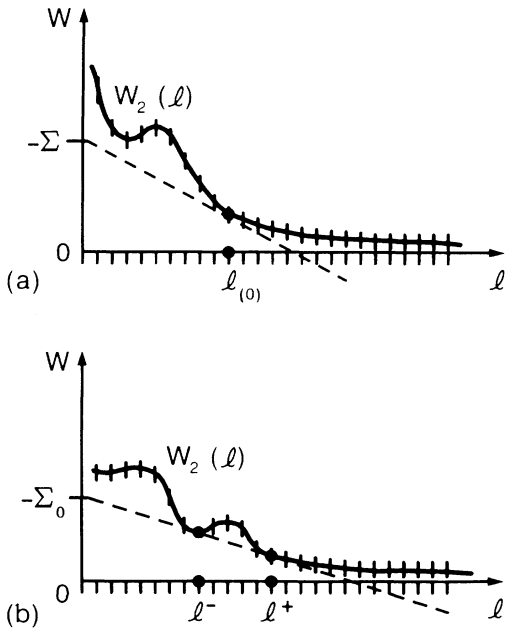

FIG. 4. (a) Example of a case (A) two-wall interaction, $W_2(l)$, which is everywhere positive. The physical domain of $W_2(l)$ is the integers $l \geq p_0$, denoted by tick marks; more generally, see (3.12) and the associated discussion. (b) Example of coexistence of two phases $[l^-], [l^+]$ when the wall tension Σ assumes the transition-point value Σ_0.

The second-order refinement of the phase diagram within the transition region of Fig. 3 appears qualitatively as shown in Fig. 5(a). The *widths*, $\Delta T_{(j)}$ or $\Delta\mu_{(j)}$, occupied by each periodic phase $[l_{(j)}]$, decay to zero as j increases. To make this more quantitative, suppose $W_2(l)$ is locally convex, so that (4.8) is satisfied, and let Σ_l^+ and Σ_l^- be the transition point values of the tension $\Sigma(T,\mu)$, say at fixed μ, bounding the phase $[l]$, i.e., locating the *pseudo-phase-boundaries* $[l]:[l+1]$ and $[l-1]:[l]$. Note that the prefix *pseudo* is used here since we are working only within the second-order approximation: the higher-order analysis of Sec. V will serve either to confirm that these boundaries represent true first-order transition loci or to reveal further structure (by way of mixed phases, etc.). The double tangent construction [see Fig. 4(b)] yields

$$\Sigma_l^{\pm} = -W_2(l) \pm l[W_2(l\pm 1) - W_2(l)] \; ; \tag{4.11}$$

hence the width of the phase $[l]$ is determined by

$$\Delta\Sigma_l \equiv \Sigma_l^+ - \Sigma_l^- = l\Delta^{(2)}W_2(l) \simeq l(d^2W_2/dl^2) \; , \tag{4.12}$$

where the approximate equality is valid if $W_2(l)$ is slowly varying and l is regarded as a continuous variable.

To illustrate this result let us suppose, in accord with the basic decay estimate (3.11), that the pair potential is given by

$$W_2(l) = U_2 w^l \; . \tag{4.13}$$

Then, accepting (4.2), the temperature width of the phase $[l_{(j)}]$ is

$$\Delta T_{(j)} \approx 2T^{\dagger} l w^{l-1} \sim l e^{-\Gamma l} \quad (l = l_{(j)}) \tag{4.14}$$

where

$$T^{\dagger} = U_2(1-w)^2/2\Sigma' \; . \tag{4.15}$$

By comparison, for a power law $W_2(l) = U_2/l^{\tau}$ one finds $\Delta T_{(j)} \approx U_2\tau(\tau+1)/\Sigma' l^{\tau+1}$.

Further details of the C-IC transition itself follow by noting that the mean value of the tension and free energy in the phase $[l]$ follow from (4.11) as

$$\bar{\Sigma}(l) \equiv \tfrac{1}{2}(\Sigma_l^+ + \Sigma_l^-)$$

$$= -\tfrac{1}{2}l[W_2(l-1) - W_2(l+1)] - W_2(l) \; , \tag{4.16}$$

$$\Delta\bar{F}_2(l) = -\tfrac{1}{2}[W_2(l-1) - W_2(l+1)] \simeq (dW_2/dl) \; . \tag{4.17}$$

If, for illustration, we again adopt (4.13) and let δT $(\equiv \delta T_l)$ be the temperature deviation in phase $[l]$ [see (4.2)] we obtain the relations

$$\delta T \approx T^{\dagger} l w^{l-1}, \quad \Delta\bar{F}_2 \approx -\Sigma' \delta T/l \; , \tag{4.18}$$

provided $l \gg 2w/(1-w^2)$. Finally, note that the *incommensurability*, $\delta\bar{q}(T,\mu)$, which measures the deviation of the mean wave vector, $\bar{q}(T,\mu)$, from the commensurate or C-phase value, $\bar{q}_C$, is given, in the phase $[l]$, simply by

$$\delta\bar{q}(T,\mu) = 2\pi/la \; . \tag{4.19}$$

Reverting the first member of (4.18) yields

$$\frac{1}{l} = \frac{a\,\delta\bar{q}}{2\pi} \approx \frac{\Gamma}{\ln(T^{\dagger}/\delta T) + \ln\ln(T^{\dagger}/\delta T) + \Gamma - \ln\Gamma} \; . \tag{4.20}$$

Note that, if we overlook the discreteness of the spacing l, this law of variation for the incommensurability agrees with the classical Frank–van der Merwe result (2.4). Likewise, the free-energy difference vanishes as

$$\Delta\bar{F}_2 \approx -\Sigma'\Gamma\,\delta T/\ln(T^{\dagger}/\delta T) \tag{4.21}$$

which corresponds to a continuous transition to the C phase $[\infty]$.

More generally, the results (4.12), (4.16), (4.17), and (4.19) imply, for case (A) pair potentials, that the C-IC transition is *quasicontinuous* with a free-energy envelope having a continuously variable slope through $T_0(\mu)$ although, in fact, the free energy displays an infinite, denumerable sequence of discrete but, asymptotically, vanishingly weak first-order transitions: see Fig. 5(b). By the same token, a plot of the mean wave vector, $\bar{q}(T,\mu)$, reveals a discrete sequence of increasingly small steps terminating in a vanishingly small "devil's last step" at the C-IC transition point: see Fig. 5(c).

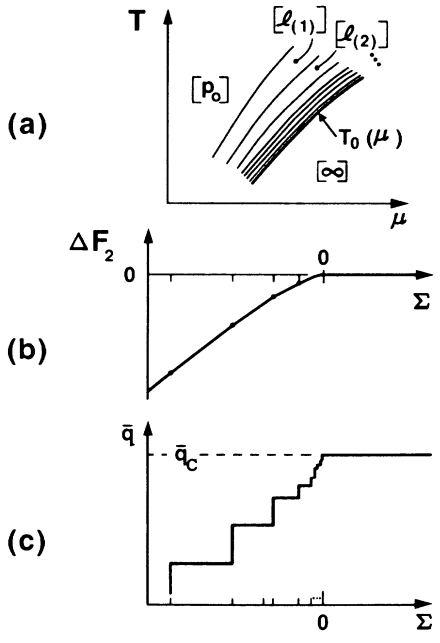

FIG. 5. (a) Refinement of the phase diagram within the transition region of Fig. 3, implied by two-wall interactions $W_2(l)$ belonging to case (A), as in Fig. 4(a). Infinitely many simple periodic phases $[l_{(j)}]$ arise between $[p_0]$ and $[\infty]$, with $p_0 < \cdots < l_{(j)} < l_{(j+1)} < \cdots$. The boundary of $[\infty]$ is the locus $\Sigma = 0$, namely, $T_0(\mu)$, of Fig. 3(a). (b) Free-energy increment, ΔF_2, *vs* the wall tension Σ; only line segments of slope $1/l_{(j)}$ are present in the graph, but their infinite number creates a quasicontinuous phase transition at $T_0(\mu)$. (c) Mean wave vector, $\bar{q}(T,\mu)$, of the phases $[l_{(j)}]$ *vs* Σ, exhibiting a devil's last step at the transition $T_0(\mu)$.

B. Case (B): First-order C-IC transition

In this case $W_2(l)$ has a unique absolute minimum of value, say, $W_{(M)}$ at $l=l_{(M)}<\infty$ as illustrated in Fig. 6. The behavior of $W_2(l)$ for $l>l_{(M)}$ has no consequences for the stable thermodynamic phases, as we will see directly; the pair potential may decay monotonically to zero or, as first stressed by Villain,[7] it may decay in an oscillatory fashion, in which situation a negative minimum must certainly exist.

It still remains true that all stable phases are simple periodic phases, $[l_{(j)}]$, determined by the graphical construction described above and illustrated in Figs. 4 and 6. When $\Sigma(T,\mu)$ exceeds the value

$$\Sigma_M=|W_{(M)}(T,\mu)|\equiv|W_2(T,\mu;l_{(M)})| \tag{4.22}$$

the optimal configuration is given by $l_{(0)}=\infty$ and the total free energy is just $F_0(T,\mu)$. As Σ falls below Σ_M, on a locus $T=T_M(\mu)$, the optimal configuration jumps discontinuously to walls at spacing

$$l_{(0)}=l_{(M)}-\Delta l \quad \text{with } \Delta l=0,1,2,\ldots\geq 0\ , \tag{4.23}$$

and the free-energy envelope decreases according to

$$\Delta\bar{F}_2\approx -W''_{(M)}\Delta l\approx -(\Sigma_M-\Sigma)/l_{(M)}\ , \tag{4.24}$$

in which

$$W''_{(M)}=\Delta^2W_2(l_{(M)})\simeq(d^2W_2/dl^2)_{l_{(M)}}\approx U_2w^{l-1}\ , \tag{4.25}$$

where the last estimate follows if we accept (4.13) for the *envelope* of $W_2(l)$. Evidently *the C-IC transition is now definitely first order in character.* Just as in case (A), the periods $l_{(j)}$ $(j=1,2,\ldots)$ of the stable phases increase monotonically with Σ, but only up to a maximum value at $j=M$; the values of $l_{(j)}$ appearing are again those for which $W_2(l)$ coincides with its convex cover $\tilde{W}_2(l)$: note that $\tilde{W}_2(l)$ now contains a level section running from $(l_{(M)}, W_{(M)})$ out to $l=\infty$.[57] The phase diagram thus appears qualitatively as in Fig. 7(a), in which the sequence of phases is cut off at $l_{(M)}$ which, in general, will depend on T (or μ). Correspondingly the staircase of wave vectors is cut off at $\bar{q}=\bar{q}_C-2\pi/l_{(M)}a$, as sketched in Fig. 7(c). In the sense that only a finite number of steps are predicted, the last step being of width

$$\Delta\Sigma_M\simeq l_{(M)}W''_{(M)}\ , \tag{4.26}$$

the graph of $\bar{q}(T,\mu)$ may be called a "harmless staircase."[7] However, it is important to recognize that this conclusion is based on a *second-order* truncation of the full free-energy expression (3.7). Inclusion of W_3, W_4, etc. may, as will be seen, reveal the appearance of further, mixed phases; indeed an infinite number of such phases might, in fact, be present[58] so that what appears to be a harmless staircase in a finite truncation would, in reality, be a true "devil's staircase."[59]

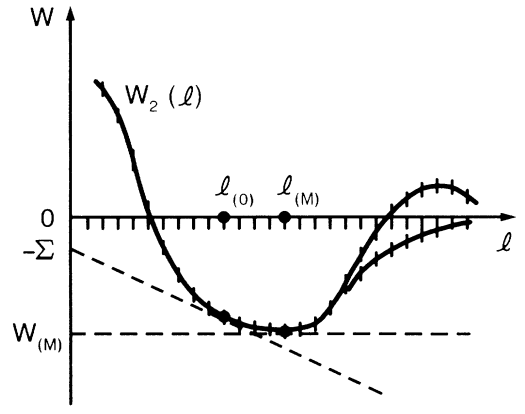

FIG. 6. Example of a case (B) two-wall interaction potential, $W_2(l)$, with a unique negative minimum at $l=l_{(M)}$. As in Fig. 4, the domain of $W_2(l)$ is the integers $l\geq p_0$ denoted by tick marks. The potential decays to zero as $l\to\infty$ but may be oscillatory.

C. Interfacial tensions

As discussed in Sec. II, between any two distinct thermodynamically stable phases, say α and β, which can physically coexist, there will be a positive interfacial tension, $\Sigma_{\alpha|\beta}$. If periodic boundary conditions are used, as we have supposed, and phase α is present over an axial interval of length L_α while β is present over length $L_\beta=L-L_\alpha$, *two* interfaces will exist in the system. If one or both α and β are modulated, domain-wall phases,

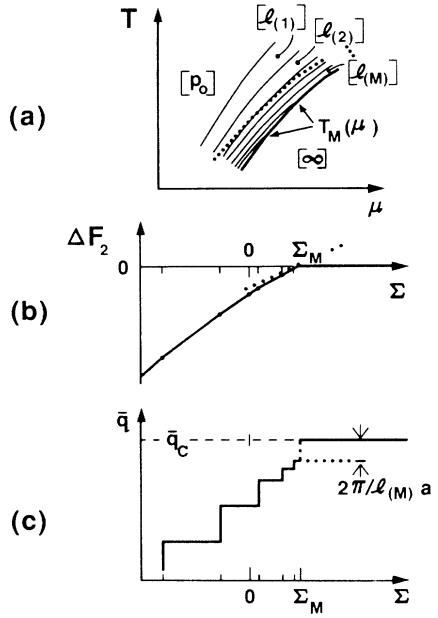

FIG. 7. (a) Refinement of the phase diagram within the transition region of Fig. 3, implied by two-wall interactions $W_2(l)$ belonging to case (B), as in Fig. 6. Only finitely many simple periodic phases $[l_{(j)}]$ arise between $[p_0]$ and $[\infty]$, with $p_0<\cdots<l_{(j)}<l_{(j+1)}<\cdots<l_{(M)}<\infty$. The dotted line represents the locus $\Sigma=0$ in Fig. 3(a), which has no special significance here. (b) Free-energy increment, ΔF_2, *vs* the wall tension Σ. As indicated by the dotted line, the C-IC transition at $\Sigma_M(T)>0$ is of first order. (c) Mean wave vector, $\bar{q}(T,\mu)$, *vs* Σ, displaying a finite jump at the transition point, $\Sigma_M(T)$.

we may use the decomposition (3.7) and calculate the interfacial tension from[60]

$$\Sigma_{\alpha|\beta}=\tfrac{1}{2}[L\,\Delta\mathcal{F}(\{\alpha|\beta|\})-L_\alpha\Delta F_\alpha-L_\beta\Delta F_\beta]\ , \quad (4.27)$$

in the limit $L_\alpha,L_\beta\to\infty$. In this expression $\Delta F_\alpha(T)$ and $\Delta F_\beta(T)$ are the, necessarily equal, incremental free energies per site of the bulk α and β phases *on* the α:β transition locus, while $\{\alpha|\beta|\}$ denotes a configuration of domain walls which describes the coexisting phases of lengths L_α and L_β.

Let us use this expression to calculate the tension $\Sigma_{[M]|[\infty]}$ between coexisting $[l_{(M)}]\equiv[M]$ and $[\infty]$ phases on the C-IC phase boundary, $T_M(\mu)$, in case (B) when the transition is first order in character. The required wall configuration can be specified by

$$l_i=l_{(M)} \quad \text{for } i=1,2,\ldots,\mathcal{N}-1$$

$$=L-(\mathcal{N}-1)l_{(M)} \quad \text{for } i=\mathcal{N}\ , \quad (4.28)$$

with $L_{[M]}=\mathcal{N}l_{(M)}$ and $L_{[\infty]}=L-L_{[M]}$. If we use the second-order truncation (4.4),(4.5), we find

$$\Sigma_{[M]|[\infty]}(T)\approx\tfrac{1}{2}\Sigma_M(T)>0\ . \quad (4.29)$$

This has the simple physical interpretation that the bounded length of phase $[M]$ contains one, terminal, domain wall which has no matching wall-interaction term, $W_2(l_{(M)})$, to cancel its free energy. Incidentally, the positivity of $\Sigma_{[M]|[\infty]}$ serves to confirm the discontinuous, first-order nature of the $[M]$:$[\infty]$ transition.

If one uses (4.27) to compute the tension $\Sigma_{[l]|[l+1]}$ between successive modulated phases [assuming for simplicity that $W_2(l)$ is locally convex] again within the pair-interaction truncation, one easily sees that the tension *vanishes identically* on the corresponding phase boundary at $\Sigma=\Sigma_l^+$ determined by (4.11). This is, clearly, a cause for concern if one believes the second-order, pseudoboundary $[l]$:$[l+1]$ is necessarily a proper first-order boundary; however, the true significance of this observation is that in order to determine the tension on the boundary and, indeed, the nature of the transition at the pseudoboundary one *must* invoke $W_3(l,l')$ and, possibly, further potentials. Accordingly we turn now to studying the role of W_3, etc., on the $[l]$:$[l+1]$ boundaries.

V. ROLE OF TRIPLET AND HIGHER-ORDER WALL INTERACTIONS

In the preceding section the total free energy, $\Delta\mathcal{F}(\{l_i\})$, of a system was studied within the two-wall or second-order truncation, $\Delta\mathcal{F}\simeq\Delta\mathcal{F}_2$: see (4.4) and Figs. 8(a) and 8(b). Only simple periodic phases $[l_{(j)}]$ were found to be stable, with free energy densities $\Delta\mathcal{F}_2=G(l_{(j)})$. On the boundary $[l_{(j)}]$:$[l_{(j+1)}]$ between two such phases, where G has degenerate minima at $l_{(j)}$ and $l_{(j+1)}$, all wall configurations $\{l_i\}$ with each l_i equal to either $l_{(j)}$ or $l_{(j+1)}$ become degenerate, according to (4.10). Close to such a phase boundary, where, say, $G(l_{(j)})\lesssim G(l_{(j+1)})$, the free-energy increase associated with changing some l_i from $l_{(j)}$ to $l_{(j+1)}$ is very small, and may be offset by the hitherto neglected $(n\geq 3)$-wall interactions W_n in $\Delta\mathcal{F}$. One must therefore examine the vicinity of each such boundary for the possible appearance of new phases not of simple periodic character. [Note, however, that these considerations do *not* apply to the final $[l_{(M)}]$:$[\infty]$ boundary arising with case (B) potentials: this boundary always represents a stable, first-order transition since, as the computation of the corresponding interfacial tension, $\Sigma_{[M]|[\infty]}$, in Sec. IV shows, one cannot construct wall configurations, $\{l_i\}$, with some l_i equal to $l_{(M)}$ and others equal to ∞ except at a non-negligible cost in free energy.]

A. Third-order truncation

For simplicity we will suppose that $W_2(l)$ is strictly convex locally and so consider only $[l]$:$[l+1]$ pseudoboundaries. When the two-wall truncation of (4.4) is extended to include the next largest term, $W_3(l,l')$, in (3.7), the free-energy density becomes

$$\Delta\mathcal{F}_3(\{l_i\})=\frac{1}{L}\sum_{i=1}^{\mathcal{N}}[\Sigma+W_2(l_i)+W_3(l_i,l_{i+1})]\ , \quad (5.1)$$

which, for a simple periodic phase, $[l]$, reduces simply to

$$\Delta\mathcal{F}_3([l])=l^{-1}[\Sigma+W_2(l)+W_3(l,l)]\ . \quad (5.2)$$

One may check first that the *shift* of the $[l]$:$[l+1]$ pseudoboundary due to the introduction of W_3 is small relative to the widths, ΔT_l and ΔT_{l+1}, of the phases $[l]$ and $[l+1]$, respectively, given by the two-wall truncation.

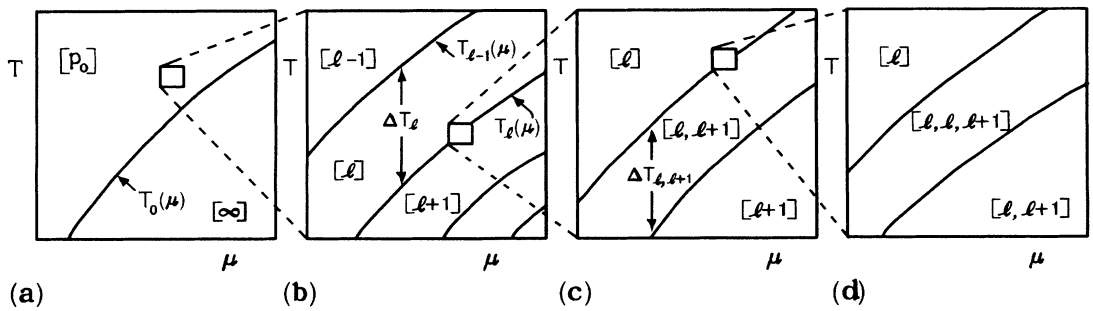

FIG. 8. Illustration of the refinement of the phase diagram by inclusion of successively higher-order multiwall interactions: (a) phase diagram for noninteracting walls (as in Fig. 3); (b) including pair interactions, $W_2(l)$, leading to simple modulated phases (as in Figs. 5 and 7); further magnifications showing mixed phases induced by appropriate (c) triplet and (d) quadruplet interactions.

Specifically, as shown in the Appendix, the fundamental decay property (3.11) implies that this shift is of order w^l times ΔT_{l+1}. The size of this narrow region between the old and new $[l]$:$[l+1]$ boundaries sets the scale over which the effects of W_3 might be significant, as illustrated in Figs. 8(b) and 8(c).

One must next examine all wall configurations $\{l_i\}$ where each l_i can be either l or $l+1$. (Recall that any *other* values of l_i have already been ruled out at the level of the two-wall truncation, and would lead to a free-energy density larger by a "large" factor of order $1/w^k$ with $k \geq 1$.) In the configuration $\{l_i\}$, we may classify each of the $\mathcal{N}$ walls $l_i \mid l_{i+1}$ by the domain widths, l_i and l_{i+1}, to its left and right, respectively: accordingly, let us associate wall types and their total numbers as follows:

$$\begin{array}{cccc} (l \mid l) & (l \mid l+1) & (l+1 \mid l) & (l+1 \mid l+1) \\ n_0 & n_+ & n_- & n_1 \end{array} \tag{5.3}$$

The periodic boundary conditions we have presupposed then imply the relations

$$n_- = n_+, \quad n_1 = \mathcal{N} - 2n_+ - n_0 \ . \tag{5.4}$$

Observe also that n_0, n_+, n_-, and n_1 must be *non-negative* and that the total system length is

$$L = \sum_{i=1}^{\mathcal{N}} l_i = (n_0 + n_+)l + (\mathcal{N} - n_+ - n_0)(l+1) \ . \tag{5.5}$$

On the $[l]$:$[l+1]$ pseudoboundary, which is determined to third order by

$$\Delta\mathcal{F}_3([l]) = \Delta\mathcal{F}_3([l+1]) \equiv \Delta F_3^{(0)} \ , \tag{5.6}$$

the free energy of the arbitrary configuration $\{l_i\}$ relative to the boundary free-energy density, $\Delta F_3^{(0)}$, can thus be written, using (5.1) and (5.2), as

$$\begin{aligned} \Delta\mathcal{F}_3(\{l_i\}) - \Delta F_3^{(0)} = L^{-1} \Big\{ & \mathcal{N}\Sigma + (n_0 + n_+)W_2(l) + (\mathcal{N} - n_+ - n_0)W_2(l+1) + n_0 W_3(l,l) \\ & + n_+[W_3(l, l+1) + W_3(l+1, l)] + (\mathcal{N} - 2n_+ - n_0)W_3(l+1, l+1) \\ & - (n_0 + n_+)l\,\Delta\mathcal{F}_3([l]) - (\mathcal{N} - n_0 - n_+)(l+1)\Delta\mathcal{F}_3([l+1]) \Big\} \\ = & -(n_+/L)[W_3(l,l) - W_3(l, l+1) - W_3(l+1, l) + W_3(l+1, l+1)] \\ \equiv & -(n_+/L)\Delta_2 W_3(l) \ . \end{aligned} \tag{5.7}$$

By virtue of the decay property (3.11), the double difference, $\Delta_2 W_3(l)$, is dominated by $W_3(l,l)$. Depending on the sign of this difference, two cases arise:

(i) If $\Delta_2 W_3(l) < 0$, the free energy is minimized by $n_+ = n_- = 0$. As a consequence, only $(l \mid l)$ and $(l+1 \mid l+1)$ walls are allowed on the boundary, which clearly means that the $[l]$:$[l+1]$ boundary is *stable* against the appearance of intervening phases and thus represents a true first-order phase boundary. This conclusion remains true even if the $(n \geq 4)$-wall interactions are included in the free energy, since these are significantly smaller.

(ii) If $\Delta_2 W_3(l) > 0$, the free energy is minimized by taking n_+ as large as possible, which is clearly achieved by alternating the spacings l and $l+1$. Consequently, the $[l]$:$[l+1]$ pseudoboundary is *unstable*: between the two simple periodic phases $[l]$ and $[l+1]$ there appears the new mixed phase $[l, l+1]$ (where the notation $[A,B]$ denotes a periodic structure with wall configurations alternating between A and B).

The second case is illustrated in Fig. 8(c). Note that the new phase $[l, l+1]$, whose stability is governed by the *three-wall* interaction $W_3(l,l')$, is constructed from its neighbors according to the branching process described in Sec. II. The reason for this specific branching rule lies, evidently, in the appearance of the factor n_+ $(=n_-)$, which effectively counts the number of $[l] \mid [l+1]$ *interfaces* in the expression (5.7) for the free-energy difference. It may be remarked that for models with only quasipairwise wall interactions, $\Phi_n(l)$, as in (3.5), the relevant wall-interaction difference becomes

$$\begin{aligned} \Delta_2 W_3(l) &= \Delta^2 \Phi_3(2l+1) \\ &\equiv \Phi_3(2l) - 2\Phi_3(2l+1) + \Phi_3(2l+2) \\ &\approx \Phi_3(2l) \ , \end{aligned} \tag{5.8}$$

which shows that the appearance of a mixed, interpolating phase is, again, really a question of the *convexity* of the potentials.[61,62]

The new boundaries $[l]$:$[l, l+1]$ and $[l, l+1]$:$[l+1]$ are, of course, determined by equating the appropriate free energies $\Delta\mathcal{F}_3$. The width, $\Delta T_{l,l+1}$, of the $[l, l+1]$ phase follows: it is of the same order as the third-order *shift* in the $[l]$:$[l+1]$ pseudoboundary as estimated in the Appendix, i.e., smaller by a factor of order w^l than the width ΔT_{l+1} of the $[l+1]$ phase, as suggested in Fig. 8(c). The corresponding incommensurability, $\delta\bar{q}_{l,l+1} = 4\pi/(2l+1)a$, interpolates between the values $\delta\bar{q}_l = 2\pi/la$ and $\delta\bar{q}_{l+1} = 2\pi/(l+1)a$ of the adjoining simple periodic phases, thus adding structure to the mean wave-vector staircases illustrated in Figs. 5 and 7.

B. Fourth-order truncation

In precisely the same manner that the $[l]$:$[l+1]$ boundary was analyzed, one must next test for the possible instability of the new mixed-phase boundaries under the inclusion of the *four-wall* interaction, W_4, in the free energy. As an illustration, the $[l]$:$[l, l+1]$ boundary will be examined. On and near this boundary, one already knows, from the discussion at the level of the three-wall truncation, that n_1, the number of $(l+1\,|\,l+1)$ walls, must vanish. To proceed, let us denote the total number of *wall pairs*, of each type by

$$\underset{n_{00}}{(l\,|\,l\,|\,l)} \quad \underset{n_{0+}}{(l\,|\,l\,|\,l+1)} \quad \underset{n_{+-}}{(l\,|\,l+1\,|\,l)} \quad \underset{n_{-0}}{(l+1\,|\,l\,|\,l)} \quad \underset{n_{-+}}{(l+1\,|\,l\,|\,l+1)} \tag{5.9}$$

The periodic boundary conditions and the constraint $n_1=0$ serve to determine all these in terms of n_{0+}, n_{0-} and n_+ alone via the relations

$$\begin{aligned} &n_{00}=n_0-n_{0+}, \quad n_{+-}=n_+ , \\ &n_{-0}=n_{0+}, \quad n_{-+}=n_+-n_{0+} ; \end{aligned} \tag{5.10}$$

none of the remaining types of wall pair can arise because $n_1=0$. The $[l]$:$[l, l+1]$ pseudoboundary, as shifted by the inclusion of W_4, is determined by the equality of the free energy

$$\Delta\mathcal{F}_4([l])=l^{-1}[\Sigma+W_2(l)+W_3(l,l)+W_4(l,l,l)] \tag{5.11}$$

with, noting that the period of $[l, l+1]$ is $2l+1$,

$$\Delta\mathcal{F}_4([l, l+1])=(2l+1)^{-1}[2\Sigma+W_2(l)+W_2(l+1)+W_3(l, l+1)+W_3(l+1, l)+W_4(l, l+1, l)+W_4(l+1, l, l+1)] , \tag{5.12}$$

which expressions, when equal, will be denoted $\Delta F_4^{(0)}$. Since $n_1=0$, the total system length L in (5.5) can be rewritten as

$$L=n_0 l+n_+(2l+1) . \tag{5.13}$$

One can now calculate the free energy of an arbitrary configuration $\{l_i\}$ relative to $\Delta F_4^{(0)}$ on the $[l]$:$[l, l+1]$ pseudoboundary as

$$\begin{aligned} \Delta\mathcal{F}_4(\{l_i\})-\Delta F_4^{(0)} &= L^{-1}\Big\{\mathcal{N}\Sigma+(n_0+n_+)W_2(l)+n_+W_2(l+1)+n_0W_3(l,l) \\ &\quad +n_+[W_3(l, l+1)+W_3(l+1, l)]+(n_0-n_{0+})W_4(l,l,l)+n_+W_4(l, l+1, l) \\ &\quad +n_{0+}[W_4(l, l, l+1)+W_4(l+1, l, l)]+(n_+-n_{0+})W_4(l+1, l, l+1) \\ &\quad -n_0 l\Delta\mathcal{F}_4([l])-n_+(2l+1)\Delta\mathcal{F}_4([l, l+1])\Big\} \\ &= -(n_{0+}/L)[W_4(l,l,l)-W_4(l, l, l+1)-W_4(l+1, l, l)+W_4(l+1, l, l+1)] \\ &\equiv -(n_{0+}/L)\Delta_2W_4(l) . \end{aligned} \tag{5.14}$$

Again, by virtue of the decay property, the difference $\Delta_2W_4(l)$ is dominated by $W_4(l,l,l)$, and two cases arise:

(i) If $\Delta_2W_4(l)<0$, the minimal free energy is given by $n_{0+}=0$, which, via (5.10), allows only the configurations $[l]$ or $[l, l+1]$ so that the $[l]$:$[l, l+1]$ boundary is *stable* against intervening phases.

(ii) If $\Delta_2W_4(l)>0$, the optimal configuration should maximize n_{0+}. Thus the $[l]$:$[l, l+1]$ boundary is *unstable* and the new mixed phase $[l, l, l+1]$ interpolates between $[l]$ and $[l, l+1]$.

The second case is illustrated in Fig. 8(d).

The analysis of the $[l, l+1]$:$[l+1]$ boundary (the only other possibility arising at the level of W_4) proceeds similarly: the free-energy difference to be minimized turns out to be the same as the last line of (5.14), but with l and $l+1$ interchanged; this also implies replacing n_{0+} there by n_{1-}, defined as the number of $(l+1\,|\,l+1\,|\,l)$ wall pairs. It follows that the $[l, l+1]$:$[l+1]$ pseudoboundary is unstable to the appearance of $[l, l+1, l+1]$ if and only if

$$\begin{aligned} \Delta_2^+W_4(l) &\equiv W_4(l, l+1, l)-W_4(l, l+1, l+1) \\ &\quad -W_4(l+1, l+1, l)+W_4(l+1, l+1, l+1) \\ &\approx W_4(l, l+1, l) \end{aligned} \tag{5.15}$$

is positive. The governing four-wall potential differences reduce to

$$\begin{aligned} &\Delta_2W_4(l)=\Delta^2\Phi_4(3l+1)\approx\Phi_4(3l) , \\ &\Delta_2^+W_4(l)=\Delta^2\Phi_4(3l+2)\approx\Phi_4(3l+1) , \end{aligned} \tag{5.16}$$

for models having only quasipairwise interactions Φ_n as in (3.5).

At this stage it is clear how the refinement of the phase diagram unfolds, as new phase boundaries are tested for stability by the inclusion of successively higher-order n-wall interactions W_n. We anticipate that the only new phases which can appear are those given by the branching process, i.e., $[A,B]$ between $[A]$ and $[B]$. In particular, if, under successive refinements of the phase diagram, $[A]$ and $[B]$ first become adjacent phases at the level of the n-wall approximation, then the appearance of $[A,B]$ should be governed, for small w, by the sign of the appropriate $(n+1)$-wall interaction W_{n+1}. If this W_{n+1} is *negative*, $[A]$:$[B]$ is a stable phase boundary and remains so under further refinements; but if this W_{n+1} is *positive*, $[A,B]$ appears as a stable interpolating phase of width smaller by a factor of order w^l, where l is the lesser of the two wall separations being mixed. It should be possible to identify for the general case what the "appropriate" W_{n+1} should be, and so to provide a demonstration of these assertions. One would then have an algorithm capable of establishing the existence of a complete devil's staircase in a given model at low temperatures (if all the appropriate W_{n+1}'s turned out to be positive). Indeed, for models with quasipairwise wall interactions, the results (5.8) and (5.16) suggest that the strict convexity of $\Phi_n(l)$ for all n should yield a complete devil's staircase. This conclusion has already been established by Bak and Bruinsma[61] (for the ground state of a one-dimensional antiferromagnetic Ising model in a field) and, more generally by Aubry.[62]

C. Interfacial tensions

We can now reopen the question of the tension of an interface, normal to the axial direction, between coexisting $[l]$ and $[l+1]$ phases when the $[l]$:$[l+1]$ boundary represents a stable first-order transition. A little reflection shows that the $\{\alpha\,|\,\beta\,|\,\}$ wall configuration required in (4.27) can be specified to third order, using the notation of (5.3), by $n_+=n_-=1$ with $L_{[l]}=l(n_0+1)$ and invoking the relations (5.4) and (5.5). The evaluation of the right-hand side of (4.27) to obtain the interfacial tension $\Sigma_{[l]\,|\,[l+1]}$ then reduces merely to a special case of the calculation in (5.7). We thus immediately obtain

$$\Sigma_{[l]\,|\,[l+1]}=-\tfrac{1}{2}\Delta_2 W_3(l)[1+O(w^l)]$$
$$\approx -\tfrac{1}{2}W_3(l,l)\sim w^{2l}\,, \tag{5.17}$$

where the correction factor allows for the neglected four-wall interactions, etc., while $\Delta_2 W_3(l)$ is defined in (5.7) and is negative since, by hypothesis, $[l]$:$[l+1]$ is here a stable first-order boundary.

A parallel analysis using (5.9), (5.10), and (5.14) with the specification $n_{0+}=n_{-0}=1$ yields the higher-order tension

$$\Sigma_{[l]\,|\,[l,\,l+1]}=-\tfrac{1}{2}\Delta_2 W_4(l)[1+O(w^l)]$$
$$\approx -\tfrac{1}{2}W_4(l,l,l)\sim w^{3l}\,, \tag{5.18}$$

and, likewise, using $n_{1-}=1$ and (5.15), we obtain

$$\Sigma_{[l,\,l+1]\,|\,[l+1]}=-\tfrac{1}{2}\Delta_2^{+} W_4(l)[1+O(w^l)]$$
$$\approx -\tfrac{1}{2}W_4(l,\,l+1,\,l)\sim w^{3l+1}\,. \tag{5.19}$$

Note, again, that these tensions are positive when the boundaries are stable.

These results for the interfacial tensions show that the testing of the stability of the $[l]$:$[l+1]$ pseudoboundary, etc., can be viewed as analogous to our original first-order analysis in which the positivity of Σ was taken as a demonstration of the stability of the C phase. One may recall in that situation, however, that attractive or case (B) wall-wall interactions could induce a transition at small positive (but nonzero) Σ: see Fig. 7. Such an instability can, in principle, also occur in the higher-order situations. Nevertheless, since the requisite interactions between the $[l]\,|\,[l+1]$ walls must be mediated by the higher-order potentials, W_n, acting between the original walls, an instability can occur only if the tensions $\Sigma_{[l]\,|\,[l+1]}$, etc., are *anomalously small,* corresponding to the transition region in Fig. 3. More concretely, "anomalously small" must mean that, owing to some cancellation of terms, $\Sigma_{[l]\,|\,[l+1]}$ is of magnitude w^{3l} or smaller, in place of the expected magnitude w^{2l} [see (5.17)] and, likewise, in higher order. This proviso concerning our earlier conclusions about the stability of the pseudoboundaries must be borne in mind in general situations: fully definitive results must, clearly, rest on more concrete information concerning the potentials W_n. To this end we now discuss how the decay estimate (3.11) can be refined.

VI. TRANSFER-OPERATOR FORMALISM

In order to gain further insight into the nature of the wall potentials, $W_n(T,\mu;l_1,l_2,\ldots,l_{n-1})$, we return to the discussion of the decay properties in Sec. III. The couplings between domain walls are effected by the same mechanisms that propagate correlations in the pure C domains. These mechanisms consist, essentially, of counterdomain fluctuations, linking the points to be correlated, with excitation energies (or free energies) determined by the underlying microscopic couplings or "interaction bonds."

To explore this picture further, consider, first, a single, flat unexcited, zero-temperature or "bare" domain wall as indicated in Fig. 9(a). At finite temperatures the domain wall will be "dressed" by excitations. When a discrete number of states may, potentially, coexist, as in Ising- and Potts-like systems, and $d>2$, the predominant excitations, as regards spatial influence, may be pictured as a "fuzz" consisting of "fingers" or "whiskers" as illustrated in Fig. 9(b). The statistical weight of a whisker stretching a distance z from the wall will be a sum of products of Boltzmann factors for the coupling bonds, say $\exp(-\Delta\varepsilon_j/k_BT)$, each product containing at least z/R_0 factors, where R_0 is the *range* of the underlying interactions, which we suppose is *finite.* The variety of individual Boltzmann factors appearing depends, clearly, on the structure of the interactions and, in particular, on the number and nature of the local heterodomain or excitation states. The magnitudes of the dominant Boltzmann factors determine the strength of correlation and, hence, are measured by the parameter w. The "free" axial propagation of such an *interaction chain* may, in analogy to

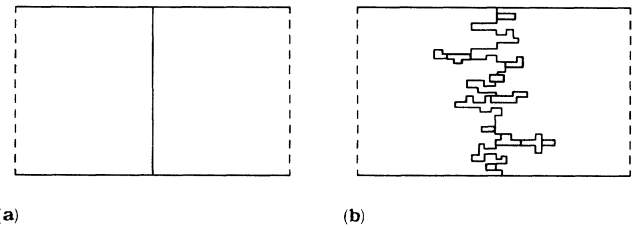

FIG. 9. Illustration of a "bare," unexcited domain wall separating distinct commensurate domains. (b) Depiction of a domain wall "dressed" with excitations: the two distinct white areas and the shaded areas indicate, for this example, three distinct types of local counterdomain fluctuations.

the bulk transfer matrix for, say, an Ising model, be generated by some transfer matrix or linear operator, say $\mathbf{V}_0$, operating on a vector space of dimensionality, say R, large enough to represent the different excitation states and their couplings to the desired level of approximation. The individual elements of $\mathbf{V}_0$ must be of magnitude w, or smaller, if one iteration of $\mathbf{V}_0$ propagates the chain axially through one lattice spacing a.

Now consider two dressed walls at separation l. They may be *linked* by a single interaction chain, as illustrated in Fig. 10(a), or by *two* or *more* interaction chains, as in Fig. 10(b). The statistical weight of the latter situations will, however, be smaller by factors w^{kl} with $k=1,2,\ldots$; and may thus be neglected in leading order (in w or l).[63] On the other hand, the propagation of the interaction chain *alone* does not yield the desired pair wall interaction, $W_2(l)$. Rather, as in the definition (3.2), the separate free energies of the individual walls must be subtracted off: the corresponding dressed configurations are illustrated in Figs. 10(c) and 10(d). Inasfar as matching excitations appear in both (a) and (c) [or in both (b) and (d)], the

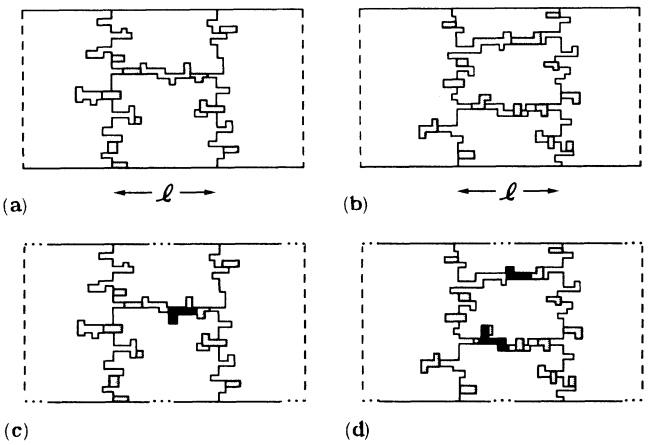

FIG. 10. Illustration of "dressed" domain walls as in Fig. 9: (a) two walls at separation l linked by a single chain of interaction bonds; (b) two walls linked by two distinct interaction chains; (c) and (d) corresponding excitation configurations of two independent walls showing overlapping fluctuations, denoted by solid black areas, which represent forbidden situations that give negative contributions to $W_2(l)$.

subtraction does not affect the propagation of the interaction chain; however, owing to the proximity of the two, otherwise independent walls some whiskers from different walls will "overlap," as indicated. These forbidden overlaps contribute *negatively* to $W_2(l)$; they may occur at any point along the interaction chain and, hence, can be incorporated into the transfer operator itself. Taking full account, likewise, of the "background" fluctuations in the C medium leads to similar extra overlap contributions. The net effect is that the true transfer operator, $\mathbf{V}$, which propagates the fully "dressed" interactions between the walls, has a more complex structure than $\mathbf{V}_0$, including, in particular, negative terms in the matrix elements (in contrast to the full bulk transfer matrix for an Ising or Potts model in which each element is a single, non-negative Boltzmann factor).

The specification of $\mathbf{V}$ which we have presented here has, of necessity, been rather sketchy owing to its generality. In subsequent papers[9] we will present details of the construction of $\mathbf{V}$ at low temperatures for the ANNNI and chiral clock models; indeed, the required matrix for the three-state chiral clock model was previously calculated in Ref. 4 (see the Appendix) but its direct connection to the wall interactions was not then realized.

Given the matrix $\mathbf{V}(T,\mu)$ for the propagation of the interactions between walls, the chain termination conditions at the walls can be described by vectors $\mathbf{a}(T,\mu)$ and $\mathbf{b}(T,\mu)$ with elements again constructed from appropriate Boltzmann factors; both $\mathbf{a}$ and $\mathbf{b}$ as well as $\mathbf{V}$ will be smooth functions of T and μ. The pair potential can finally be expressed as[10]

$$W_2(l)\approx \mathbf{a}^\dagger \mathbf{V}^l \mathbf{b} , \tag{6.1}$$

in which the dagger denotes the appropriate transposition or duality operation. Note that the corrections of relative order w^l due to pairs of interaction chains, etc., have been neglected here.

The three-wall and higher-order interactions can be generated similarly. The new feature is that, owing to the definition of W_3, W_4, etc., the single dominant interaction chain must *span* the full extent, $l_{\rm tot}=l_1+l_2+\cdots+l_{n-1}$, of the potential. However, when the interaction chain propagates *through* the *intermediate* walls somewhat different local excitations and couplings must be involved. These can be accounted for (as is most readily seen in explicit calculations[9]) by a modified transfer operator, say $\mathbf{C}(T,\mu)$, again a smooth function of T and μ. Then the *multi*wall interactions can be expressed as

$$W_3(l,l')\approx \mathbf{a}^\dagger \mathbf{V}^l \mathbf{C} \mathbf{V}^{l'} \mathbf{b} , \tag{6.2}$$

$$W_4(l,l',l'')\approx \mathbf{a}^\dagger \mathbf{V}^l \mathbf{C} \mathbf{V}^{l'} \mathbf{C} \mathbf{V}^{l''} \mathbf{b} , \tag{6.3}$$

etc., where, again, the multichain contributions of orders $w^{l+l'}$ or $w^{l+l'+l''}$ times the leading terms have been neglected. (It may be more convenient, in practical calculations, to replace the powers $l',l'',\ldots$ by $l'-p_0,l''-p_0,\ldots$ to allow for the width of the intermediate walls represented by $\mathbf{C}$.)

Now the operators or matrices $\mathbf{V}$ are *not*, in general, symmetric or Hermitian: Nevertheless, with the aid of the Jordan normal form or its analogs they will have a

spectral resolution entailing the eigenvalues of $\mathbf{V}$, say, λ_r $(r=1,2,\ldots,R)$. For simplicity at this point we will suppose that the corresponding eigenvectors form a complete set. Then we may rewrite (6.1)–(6.3) in the more explicit forms[10]

$$W_2(T,\mu;l)\approx \sum_{r=1}^{R} A_r(T,\mu)[\lambda_r(T,\mu)]^l , \tag{6.4}$$

$$W_3(T,\mu;l,l')\approx \sum_{r,r'=1}^{R} A_{r,r'}(T,\mu)\lambda_r^l\lambda_{r'}^{l'} , \tag{6.5}$$

and so on. Note that the variation of the eigenvalues λ_r and amplitudes $A_r, A_{r,r'}, \ldots$ with T and μ is smooth provided no eigenvalue degeneracies are encountered; in that case, however, the dependence of the λ_r, A_r, $A_{r,r'}$, etc. will, in general, be singular but of a character determined by the order of the degeneracy and the fact that the matrices $\mathbf{V}$ and $\mathbf{C}$ and vectors $\mathbf{a}$ and $\mathbf{b}$ are smooth functions of T and μ. An illustration of this principle is provided in the next section where we analyze a situation entailing a crossing of eigenvalues.

The expressions (6.4) and (6.5) reveal the characteristic forms of decay that should be anticipated. Thus, in the simplest situation one eigenvalue, say, $\lambda_1=\exp(-\Gamma_1)$, strongly dominates and yields

$$W_2(l)\simeq A_1 e^{-\Gamma_1 l}, \quad W_3(l,l')\simeq A_{11}e^{-\Gamma_1(l+l')} , \tag{6.6}$$

etc. in direct accord with the fundamental decay property (3.11). When A_1 is positive one has a case (A) pair potential; the sign of A_{11} then determines, via (5.7), the stability of the $[l]$:$[l+1]$ boundaries or the appearance of the mixed phase $[l, l+1]$.

If a pair of complex eigenvalues, $\lambda_\pm=\exp(-\Gamma_0\pm i\omega)$, dominates, one obtains the forms

$$W_2(l)\simeq A_0 e^{-\Gamma_0 l}\sin[\omega(l+\epsilon)] , \tag{6.7}$$

$$W_3(l,l')\simeq e^{-\Gamma_0(l+l')}\{A_+\sin[\omega(l+l'+\epsilon_+)]+A_-\sin[\omega(l-l'+\epsilon_-)]\} , \tag{6.8}$$

$$\begin{aligned} W_4(l,l',l'')\simeq e^{-\Gamma_0(l+l'+l'')}\{ & A_{++}\sin[\omega(l+l'+l''+\epsilon_{++})] \\ & + A_{+-}\sin[\omega(l+l'-l''+\epsilon_{+-})]+A_{-+}\sin[\omega(l-l'+l''+\epsilon_{-+})] \\ & + A_{--}\sin[\omega(l-l'-l''+\epsilon_{--})]\} , \end{aligned} \tag{6.9}$$

and so on. The oscillatory form of $W_2(l)$ implies a case (B) situation with an absolute minimum at $l_{(M)}$ between $l=\pi/\omega$ and $l=3\pi/2\omega$ for $A_0>0$, or less than $\pi/2\omega$ for $A_0<0$. Note that $W_3(l,l)$, which determines the stability of the simple periodic boundaries, is proportional to $A_+\sin(2\omega l+\omega\epsilon_+)+B$ which varies strongly with l yielding, when $|A_+|>|B|=|A_-\sin\omega\epsilon_-|$, alternating regions in which mixed phases do *or* do not appear. Such a situation is found in concrete calculations for the ANNNI model.[9,10]

When two real eigenvalues are comparable in magnitude one has forms

$$W_2(l)\simeq A_1 e^{-\Gamma_1 l}+A_2 e^{-\Gamma_2 l} , \tag{6.10}$$

$$\begin{aligned} W_3(l,l')\simeq e^{-\Gamma_1(l+l')}(& A_{11}+A_{21}e^{-\Delta\Gamma l}+A_{12}e^{-\Delta\Gamma l'} \\ & + A_{22}e^{-\Delta\Gamma(l+l')}) , \end{aligned} \tag{6.11}$$

etc, with $\Delta\Gamma\equiv\Gamma_2-\Gamma_1>0$. If A_1 and A_2 are both positive, $W_2(l)$ embodies a simple case (A) situation. However, if A_1 is negative but $A_2+A_1>0$, the potential has a simple minimum at $l_{(M)}\simeq\ln(\Gamma_2 A_2/\Gamma_1|A_1|)/\Delta\Gamma$ and the case (B) analysis applies. As T and μ vary one may, evidently, have a changeover from case (B) to case (A): this yields a *quasitricritical point* which we analyze further in the next section. Such a thermodynamic feature is realized in explicit calculations for the three-state chiral clock model[9,10] and might well arise in real systems also.

Finally, we mention a rather special *degenerate* case which, nonetheless, arises, in leading approximation, in models like the ANNNI model.[10] This is epitomized by a transfer matrix of the lower triangular form

$$\mathbf{V}_1=\begin{bmatrix}\lambda_0 & 0\\ v_0 & \lambda_0\end{bmatrix} \quad (v_0\neq 0) , \tag{6.12}$$

which possesses a unique eigenvalue, λ_0, and only one eigenvector, namely, $\begin{bmatrix}0\\1\end{bmatrix}$. The formula (6.4) does not apply but from (6.1) one finds the form

$$W_2(l)=(A_0 l+A_1)e^{-\Gamma_0 l} . \tag{6.13}$$

If A_0 and A_1 are positive, one clearly has a realization of case (A), with an infinite number of simple periodic phases and a quasicontinuous C-IC transition. If $\mathbf{V}_1$ were the exact transfer matrix there would be no more to say; if however, as will be typical in model calculations, it represents a leading approximation, corrections, say of higher order in w, should be present. In that case one must expect that the eigenvalue degeneracy entailed in (6.12) will be *broken*. The resulting perturbed and/or enlarged matrix[9] will have two eigenvalues λ_+ and λ_- corresponding to λ_0 (and two independent eigenvectors). If λ_+ and λ_- are real, the resulting potential, $W_2(l)$, will then take the form (6.10) but will be qualitatively similar to (6.13) and, hence, of the same case (A) character although differing quantitatively to a small extent. Conversely, it may well happen, as we find in the ANNNI model,[9,10] that the original eigenvalue, λ_0, splits under the higher-order perturbation into a *complex conjugate pair*. Then the oscillatory expression (6.7) applies and $W_2(l)$ actually realizes case (B) with a bounded number of simple periodic phases! Thus the original conclusion of a

quasicontinuous C-IC transition is falsified by the inclusion of the higher-order corrections: the details of this mechanism and the phase diagrams, etc., that may result in these circumstances will be seen in our explicit analysis of the ANNNI model.

VII. THE QUASITRICRITICAL POINT

An instructive application of the general domain-wall interaction formalism we have developed is to study the phenomenon of *quasitricriticality* in which the nature of the C-IC transition in the phase diagram switches, as T or μ varies, from quasicontinuous with a "devil's last step" [case (A)] to first order with a finite jump in the incommensurability at the transition [case (B)].

To analyze a quasitricritical point and its vicinity it suffices to suppose that only two eigenvalues of the transfer operator, $\mathbf{V}$, are important and thus to consider the simplified situation in which the pair wall interaction is represented by

$$W_2(l)=[1,1]\mathbf{V}^l\begin{bmatrix}B_1\\B_2\end{bmatrix}, \tag{7.1}$$

in which $\mathbf{V}$ is a 2×2 matrix and B_1 and B_2 are smoothly varying functions of T and μ. [The representation of $\mathbf{a}^\dagger$ in (6.1) by the constant vector [1,1] will be of no consequence.] We shall examine quasitricriticality in a general framework which, however, is actually realized in our study of the three-state chiral clock model,[9,10] where the lowest-energy excitations contributing to $W_2(l)$ give $\mathbf{V}$ with the diagonal form

$$\mathbf{V}=\lambda_0\begin{bmatrix}1+\delta & 0\\ 0 & 1-\delta\end{bmatrix}, \tag{7.2}$$

in which λ_0, which is of order w, and δ are smooth functions of T and μ. This yields

$$W_2(l)=\lambda_0^l[B_1(1+\delta)^l+B_2(1-\delta)^l], \tag{7.3}$$

which parallels (6.10) of the general discussion: as observed there, if the amplitudes B_i are of opposite sign and satisfy the relations

$$B_1>0,\quad B_2<0,\quad B_1>|B_2|, \tag{7.4}$$

the *crossing* of the eigenvalues $\lambda_\pm=\lambda_0(1\pm\delta)$ as δ passes through zero causes $W_2(l)$ to switch from case (B) behavior for $\delta<0$ to case (A) behavior for $\delta>0$. Thus, as illustrated in Fig. 11, $\delta=0$ represents a quasitricritical point. On approaching this point from the first-order side where $\delta<0$, the maximum interwall separation, $l_{(M)}$, determined by the minimum of $W_2(l)$, diverges with a *simple-pole* singularity, according to

$$l_{(M)}\approx\tfrac{1}{2}\ln(B_1/|B_2|)/|\delta|. \tag{7.5}$$

The qualitative appearance of the modulated phases in the vicinity of a quasitricritical point in the (T,μ) diagram can be seen in Fig. 1 of Ref. 10 (see also Ref. 9).

The quasitricritical point at $\delta=0$ is evidently a special point where the transfer matrix $\mathbf{V}$ of (7.2) displays a high degree of symmetry. One should anticipate that perturbations due to higher-energy excitations, etc., will spoil this special symmetry and, perhaps, thus alter the character of the quasitricriticality. As implicit in the discussion of Sec. VI, inclusion of higher-energy excitations in the calculation of $W_2(l)$ will generally require that the dimension of $\mathbf{V}$ be increased, but it will be possible in general to obtain the leading behavior by projecting the enlarged matrix back to a 2×2 matrix with slightly modified elements.[9] We shall therefore consider a general perturbation under which (7.2) becomes

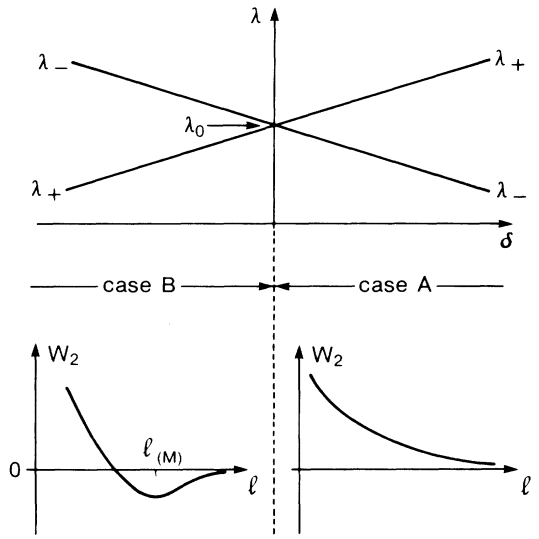

FIG. 11. Variation of transfer-matrix eigenvalues to leading order near a quasitricritical point at $\delta=0$. The corresponding two-wall interaction $W_2(l)$ [see (7.1)–(7.4)] has a negative minimum for $\delta<0$ [case (B) behavior] but not for $\delta>0$ [case (A)]; hence the C-IC transition changes from first order to quasicontinuous.

$$\mathbf{V}=\lambda_0\begin{bmatrix}1+\delta & h_++g_+\delta\\ h_-+g_-\delta & 1-\delta\end{bmatrix}. \tag{7.6}$$

This is, in fact, the most general form of perturbation, since any changes in the diagonal elements can be absorbed into redefinitions of λ_0 and δ, while the off-diagonal elements contain terms which are separately even and odd under change of the sign of δ. Since these perturbations arise from higher-order excitation processes, one expects to have

$$|h_\pm|,|g_\pm|=O(w)\ll1. \tag{7.7}$$

The analysis of (7.6) that follows reveals that this general perturbation does *not* destroy the quasitricritical point implied by the ideal form (7.3). Rather, a limited range of possibilities emerges: either the quasitricritical point is simply *shifted* to some nonzero value of δ, or, additionally, there may appear a new *pair* of conjugate quasitricritical points bounding a small region of case (B) behavior but, otherwise, lying wholly within the case (A) regime. However, in the generic case, the simple pole divergence

(7.5) *is* modified, yielding either a logarithmic or square-root divergence: see (7.25)–(7.27), below.

Now the eigenvalues of the perturbed matrix (7.6) can be written

$$\tilde{\lambda}_{\pm}=\lambda_0[1\pm s(\delta)] , \tag{7.8}$$

where the (positive or negative) variable which will stand in for δ is

$$s^2(\delta)=(1+g_+g_-)(\delta-\delta_0)^2+Q , \tag{7.9}$$

in which the small *shift parameters* are

$$\delta_0\equiv-\frac{g_-h_++g_+h_-}{2(1+g_+g_-)} \tag{7.10}$$

and

$$Q\equiv\frac{h_+h_--\frac{1}{4}(g_-h_+-g_+h_-)^2}{1+g_+g_-} . \tag{7.11}$$

Note that, for δ in the vicinity of δ_0, (7.7) implies that s^2 is small, namely, of order $h_{\pm}^2=O(w^2)$. One may therefore rewrite the eigenvalues (7.8) in a more convenient form as

$$\tilde{\lambda}_{\pm}=\tilde{\lambda}_0e^{\pm\gamma s} , \tag{7.12}$$

with

$$\tilde{\lambda}_0=\lambda_0[1-\tfrac{1}{2}s^2+O(s^4)], \quad \gamma=1+O(s^2) . \tag{7.13}$$

The new form of the two-wall interaction following from these perturbed eigenvalues is

$$W_2(l)=D_1\tilde{\lambda}_+^l+D_2\tilde{\lambda}_-^l , \tag{7.14}$$

in which the new amplitudes D_i are most readily found by matching this expression with $l=0$ and $l=1$ to the corresponding results computed directly from (7.6) and (7.1). This leads to

$$W_2(l)=\tilde{\lambda}_0^l\left[\bar{B}(e^{\gamma sl}+e^{-\gamma sl})+\frac{C(\delta)}{s(\delta)}(e^{\gamma sl}-e^{-\gamma sl})\right] , \tag{7.15}$$

where, recalling the relations (7.4), we have

$$\bar{B}\equiv\tfrac{1}{2}(B_1+B_2)>0, \quad C(\delta)=C_0+C_1\delta , \tag{7.16}$$

$$\begin{aligned} C_0&\equiv\tfrac{1}{2}(B_1h_-+B_2h_+) , \\ C_1&\equiv\tfrac{1}{2}[B_1(1+g_-)-B_2(1-g_+)]>0 . \end{aligned} \tag{7.17}$$

Having obtained a general expression for $W_2(l)$, we wish to determine the conditions under which it belongs to, say, case (B). Since the criterion for that case is that W_2 possess a negative minimum, and since W_2 decays to zero as $l\to\infty$, it follows that W_2 belongs to case (B) if and only if it possesses zeros. There are two cases to consider in (7.15): (i) if $s^2<0$, so that $s=i\,|\,s\,|$ is pure imaginary, one obtains

$$W_2(l)=2\tilde{\lambda}_0^l\left[\bar{B}\cos(\gamma\,|\,s\,|\,l)+\frac{C}{|\,s\,|}\sin(\gamma\,|\,s\,|\,l)\right] \tag{7.18}$$

which *always* has a zero, at l given by

$$\tan(\gamma\,|\,s\,|\,l)=-\bar{B}\,|\,s\,|/C ; \tag{7.19}$$

alternatively, (ii) if $s^2>0$, so that one may take $s>0$ real, one can write

$$W_2(l)=2\tilde{\lambda}_0^l\left[\bar{B}\cosh(\gamma sl)+\frac{C}{s}\sinh(\gamma sl)\right] \tag{7.20}$$

which has a zero at l given by

$$\tanh(\gamma sl)=-\bar{B}s/C , \tag{7.21}$$

if and only if

$$C<0 \text{ and } C<-\bar{B}(s^2)^{1/2} . \tag{7.22}$$

These results identify a locus of potential quasitricriticality in the (s^2,C) plane, and thence, via (7.9)–(7.11), (7.16), and (7.17), etc., in the (T,μ) plane, which separates the regimes in which $W_2(l)$ exhibits case (A) or case (B) behavior, respectively. This locus is exhibited on Fig. 12. On the (s^2,C) plane, one can also plot the principal "trajectory" of the system as parametrized by δ: according to

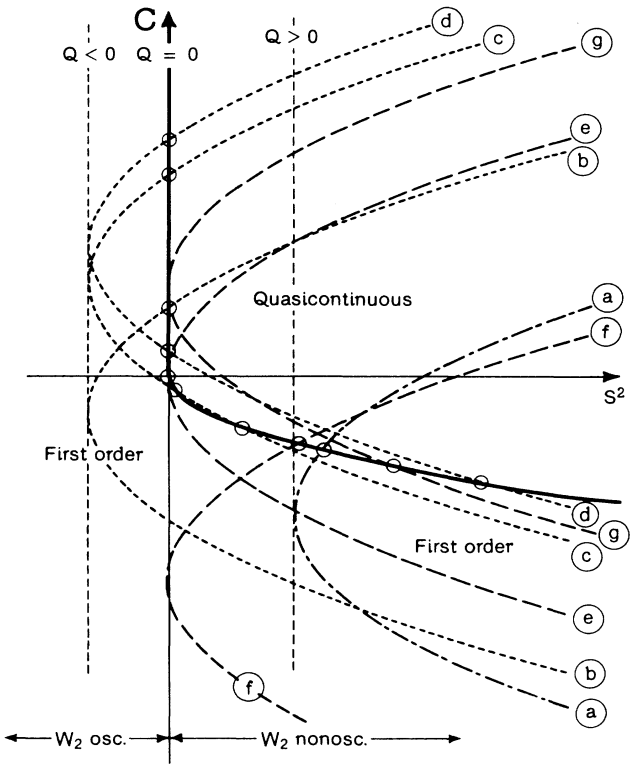

FIG. 12. Characterization of quasitricriticality under a general perturbation (see text for definitions of the parameters s^2 and C). The heavy curve composed of the $s^2=0$ axis for $C>0$ and a parabola for $C<0$ is the locus of potential quasitricriticality, separating regimes of first-order and quasicontinuous C-IC transitions. The trajectory of the system is also a parabola in this plane, of which the dash-dotted, dotted, and dashed curves (a)–(g) represent examples: the labeling corresponds to the classification in the text. Quasitricritical points occur at those points (circled) where the system trajectory crosses the locus of potential quasitricriticality. Within the first-order regime, the wall-wall pair interaction potential $W_2(l)$ is oscillatory for $s^2<0$ but nonoscillatory (a sum of two exponentials) for $s^2>0$. The divergence of the maximum period, $l_{(M)}$, on approach to quasitricriticality from the first-order regime is logarithmic for $C<0$, as a square root for $C>0$, and as either a square root or a simple pole for $C=0$ (see Tables I and II).

(7.9) and (7.16), this is the parabola

$$s^2(\delta)-Q=(1+g_+g_-)[C(\delta)-C(\delta_0)]^2/C_1^2 \ . \quad (7.23)$$

Several of these parabolae, corresponding to different locations for the vertex $[s^2=Q,\ C=C(\delta_0)]$, are shown in Fig. 12. A quasitricritical point occurs whenever the system trajectory crosses the locus of potential quasitricriticality where $W_2(l)$ switches between case (A) and case (B) behavior. All possible situations are thus readily categorized. However, it is important to note, as one may verify from (7.22) and (7.23), that the system trajectory is always a *broader* parabola than that defining the locus of potential quasitricriticality in the half-plane $C<0$, *except* in "pathological" cases in which the original amplitudes are of widely differing magnitudes and satisfy

$$B_1/B_2 \lesssim 2/g_- = O(w^{-1}) \ . \quad (7.24)$$

Barring this unlikely circumstance, only the following situations can occur (the labels corresponding to those of the system trajectories drawn on Fig. 12):

(i) if $Q>0$, then

(a) under the perturbations there continues to be only a single *quasitricritical point* (QTP), at $C<0$, which, in general, occurs at some shifted, nonzero value $\delta=\delta_c$;

(ii) if $Q<0$, then *either*

(b) there is again only a single QTP, which may be either at $C<0$ or $C\geq 0$; *or*

(c) there are *two* QTP's at $C<0$ and one QTP at $C>0$; *or*

(d) there is one QTP at $C<0$ and two QTP's at $C\geq 0$;

(iii) if $Q=0$, then *either*

(e) there is a single QTP at $C=0$; *or*

(f,g) there is a single QTP at $C<0$.

The quasitricritical points occurring at $C<0$ are of somewhat different character from those occurring at $C\geq 0$, since on approaching the former from the case (B) regime of first-order C-IC transitions, $W_2(l)$ is nonoscillatory, as given by (7.20), whereas the latter quasitricritical points have $W_2(l)$ oscillating in the case (B) regime, as in (7.18). This difference is reflected in the manner in which the maximum wall separation, $l_{(M)}$, *diverges* as the quasitricritical point is approached. When $W_2(l)$ is nonoscillatory ($C<0$), $l_{(M)}$ diverges only *logarithmically* at the quasitricritical point at $\delta=\delta_c$ according to

$$l_{(M)} \approx \tfrac{1}{2}[\bar{B}/|C(\delta_c)|]\ln|\delta-\delta_c|^{-1} \ ; \quad (7.25)$$

but when $W_2(l)$ is oscillatory ($C>0$), $l_{(M)}$ exhibits the *square-root* singularity

$$l_{(M)} \approx \pi[2(1+g_+g_-)(\delta_0-\delta_c)(\delta-\delta_c)]^{-1/2} \ , \quad (7.26)$$

as $\delta\rightarrow\delta_c$. Provided $Q\neq 0$, the special quasitricritical point at $C=0$ is again characterized by a square-root singularity, with $l_{(M)}$ varying as one-half the right-hand side of (7.26). When $Q=0$, as in trajectory (e) of Fig. 12, the special quasitricritical point at $C=0$ has the same simple-pole singularity found for the original, unperturbed situation [compare with (7.5)], namely,

$$l_{(M)} \approx \frac{\tanh^{-1}[(\bar{B}/C_1)(1+g_+g_-)^{1/2}]}{(1+g_+g_-)^{1/2}(\delta_0-\delta)} \ . \quad (7.27)$$

From the appropriate asymptotic form of $l_{(M)}$, one can also check the *shape* of the C-IC phase boundary through the quasitricritical point in the (δ,T) plane: see Fig. 13. As discussed in Sec. IV, the boundary of the C phase, $[\infty]$, is given in the quasicontinuous regime simply by the locus, $T=T_0(\delta)$, on which the surface tension, Σ, vanishes. In the first-order regime, however, the C phase boundary, $T=T_M(\delta)$, is shifted away from $T_0(\delta)$ by an amount, ΔT, which is determined according to (4.2) and (4.22) as

$$\Delta T \approx |W_2(l_{(M)})|/\Sigma' \ . \quad (7.28)$$

Now, insofar as $W_2(l_{(M)})$ is dominated by the exponential factor $\tilde{\lambda}_0^{\,l_{(M)}}$ [recall (7.18) or (7.20)], one would expect that a *simple-pole* or *square-root* divergence of $l_{(M)}$, as in (7.5), (7.26), or (7.27), causes the phase-boundary shift, ΔT, to vanish *exponentially,* whence the C phase boundary *continues smoothly* through the quasitricritical point. A *logarithmic* divergence of $l_{(M)}$, however, as in (7.25), should produce a *power-law* behavior in ΔT,

$$\Delta T \sim |\delta-\delta_c|^{\phi} \ , \quad (7.29)$$

with an exponent

$$\phi \approx \tfrac{1}{2}(\bar{B}\ln\tilde{\lambda}_0^{-1})/|C(\delta_c)| \quad (7.30)$$

which is *nonuniversal,* depending on the particular perturbation amplitudes, $g_\pm$ and $h_\pm$, through $C(\delta_c)$ [recall (7.16) and (7.17)]. Note that, since $\tilde{\lambda}_0 \approx \lambda_0 = O(w)$ is a small Boltzmann factor, ϕ will tend to be a large exponent, thereby again imparting a high degree of smoothness to the C phase boundary through the quasitricritical point.

These expectations have been verified by explicit evalua-

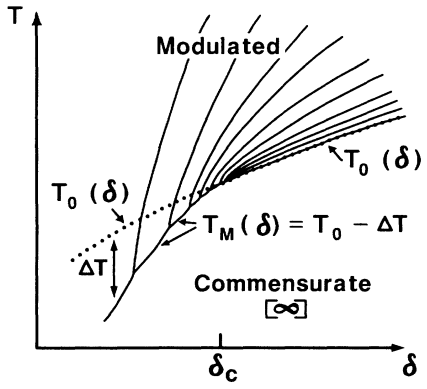

FIG. 13. Illustration of the C-IC phase boundary in the vicinity of a quasitricritical point at $\delta=\delta_c$. On the quasicontinuous side, the C phase boundary is given by the locus, $T=T_0(\delta)$, on which the wall surface tension, Σ, vanishes; on the first-order side, the C phase boundary, $T=T_M(\delta)$, differs from $T_0(\delta)$ by a shift, ΔT, which vanishes either exponentially or as a power law as the quasitricritical point is approached: see Tables I and II.

tion of (7.28); detailed amplitudes of the various asymptotic forms are collected and displayed in Tables I and II, which summarize all the types of quasitricriticality that we have discussed.

Finally, notice that *within* the case (B) regime of first-order C-IC transitions, it is possible that $W_2(l)$ will change between the oscillatory form of (7.18) and the nonoscillatory form of (7.20), as in trajectories (b) and (c) of Fig. 12 that cross the ray $s^2=0$, $C<0$. One can, however, check that $l_{(M)}$ continues smoothly across this ray, being given, in the vicinity, by

$$l_{(M)} \approx (\bar{B}/|C|) - (\ln\tilde{\lambda}_0)^{-1} . \tag{7.31}$$

This completes our analysis of quasitricriticality on the C-IC transition locus. Unlike ordinary bulk tricriticality, as observed, e.g., in ^{3}He-^{4}He mixtures or in metamagnets, three distinct forms of asymptotic singularity may arise although only two, the logarithmic and square-root forms, should be generic.

VIII. CONCLUSIONS

We have explored features of the phase diagrams of systems exhibiting uniaxial modulated phases, by focusing on the interactions among the domain walls. A systematic method has been outlined for determining the general features of these interactions, and their effects on the topology of the phase diagram. This approach may be useful for modeling a wide variety of physical systems at temperatures sufficiently low that the walls are well defined and pinned to the underlying lattice.

Especially noteworthy is the demonstration that although the *pair* potentials, $W_2(l)$, are responsible for stabilizing the *simple periodic* phases, $[l]$, and determining the locus of the C-IC transition, it is the *many-body* potentials, $W_n(l_1,l_2,\ldots)$ for $n\geq 3$, that control the appearance of higher-order or *mixed* phases $[l,l+1]$, etc. Moreover, for systems with short-range interactions, a transfer operator method reveals the general character of the $W_n(l_1,l_2,\ldots)$. Using this approach, asymptotically exact low-temperature expressions for $W_2(l)$, $W_3(l,l')$, ... are calculable for a variety of statistical mechanical models: a detailed account will be given in subsequent papers.[9]

Finally, we have noted the existence and studied the properties of a novel *quasitricritical point* on the C-IC transition boundary, governed by the functional form of the two-wall interaction potential $W_2(l)$. This is a feature which might be detected by further experiments on systems with uniaxial modulated phases.

ACKNOWLEDGMENTS

We wish to thank W. Selke for informative conversations and correspondence. The support of the National Science Foundation, principally through the Materials Science Center at Cornell University,[64] is gratefully acknowledged. The hospitality of the Aspen Center for Physics, where the writing of this paper was completed, is also appreciated.

APPENDIX: PHASE BOUNDARY SHIFTS

The purpose of this Appendix is, first, to justify the claim in Sec. IV, that the variation of $W_2(l)$ with the parameters T, μ, etc., can be ignored in refining the phase diagram near the first-order $[p_0]$:$[\infty]$ pseudoboundary. In particular, imagine traversing the phase diagram by increasing T at fixed μ. Suppose the stable phase is allegedly $[l]$, bounded by $[l+1]$ at $T=T_l(\mu)$ and $[l-1]$ at $T=T_{l-1}(\mu)$ [see Fig. 8(b)]. If, as asserted, these boundaries are to be insensitive to the variation of $W_2(T,\mu;l)$ with T across the phase width

$$\Delta T_l \equiv T_{l-1}(\mu) - T_l(\mu) , \tag{A1}$$

it is sufficient to establish

$$\Delta_T W_2 \equiv |W_2(T_{l-1};l) - W_2(T_l;l)| \ll \Delta_l W_2 \equiv |W_2(T_l;l) - W_2(T_l;l+1)| , \quad \Delta_{l-1} W_2 . \tag{A2}$$

TABLE I. The various types of quasitricritical points, as characterized by the form of the two-wall interaction potential, $W_2(l)$, on the first-order side of the C-IC phase boundary (see Fig. 13). On the approach to the quasitricritical point at $\delta=\delta_c$, the functional form of $W_2(l)$ [as well as the sign of the associated amplitude $C(\delta_c)$] determines both the divergence of the maximum interwall spacing, $l_{(M)}$, and the vanishing of the difference, ΔT, between the actual first-order C-IC boundary and the potential quasicontinuous C-IC transition locus [see (7.28)]. The coefficients a_i and b_i are listed in Table II.

Form of $W_2(l)$		Asymptotic form of $l_{(M)}$ $(\to\infty)$	Asymptotic form of ΔT $(\to 0)$
Unperturbed nonoscillatory [Eq. (7.3)]		$a_1\lvert\delta-\delta_c\rvert^{-1}$ $(\delta_c\equiv 0)$	$b_1\lvert\delta-\delta_c\rvert\lambda_0^{a_1\lvert\delta-\delta_c\rvert^{-1}}$ $(\delta_c\equiv 0)$
Perturbed nonoscillatory	$C(\delta_c)<0$	$a_2\ln\lvert\delta-\delta_c\rvert^{-1}$	$b_2\lvert\delta-\delta_c\rvert^{\phi}$
[Eq. (7.20)]	$C(\delta_c)=0$	$a_3\lvert\delta-\delta_c\rvert^{-1}$	$b_3\lvert\delta-\delta_c\rvert\tilde{\lambda}_0^{a_3\lvert\delta-\delta_c\rvert^{-1}}$
Perturbed oscillatory	$C(\delta_c)>0$	$a_4\lvert\delta-\delta_c\rvert^{-1/2}$	$b_4\tilde{\lambda}_0^{a_4\lvert\delta-\delta_c\rvert^{-1/2}}$
[Eq. (7.18)]	$C(\delta_c)=0$	$a_5\lvert\delta-\delta_c\rvert^{-1/2}$	$b_5\lvert\delta-\delta_c\rvert^{1/2}\tilde{\lambda}_0^{a_5\lvert\delta-\delta_c\rvert^{-1/2}}$

TABLE II. Coefficients of the asymptotic forms listed in Table I, in terms of the parameters defined in Sec. VII of the text.

$a_1=\frac{1}{2}\ln(B_1/\lvert B_2\rvert)$	$b_1=2(B_1\lvert B_2\rvert)^{1/2}/(\Sigma'\kappa_0)$
$a_2=\frac{1}{2}\bar{B}/\lvert C(\delta_c)\rvert$	$\phi=\frac{1}{2}[1+\bar{B}\tilde{\kappa}_0/\lvert C(\delta_c)\rvert]$
	$b_2=[4\lvert C(\delta_c)\rvert/\Sigma'\tilde{\kappa}_0]\left[\frac{C_1\lvert C(\delta_c)\rvert+\bar{B}^2 g(\delta_c-\delta_0)}{2\lvert C(\delta_c)\rvert^2}\right]^{\phi}$
$a_3=g^{-1/2}\tanh^{-1}(\bar{B}g^{1/2}C_1^{-1})$	$b_3=2(C_1^2-\bar{B}^2 g)^{1/2}/(\Sigma'\tilde{\kappa}_0)$
$a_4=\pi(2g\lvert\delta_0-\delta_c\rvert)^{-1/2}$	$b_4=2C(\delta_c)/(\Sigma'\tilde{\kappa}_0)$
$a_5=\frac{1}{2}a_4$	$b_5=2\pi\bar{B}/(a_4\Sigma'\tilde{\kappa}_0)$

$$\kappa_0\equiv\ln\lambda_0^{-1},\quad \tilde{\kappa}_0\equiv\ln\tilde{\lambda}_0^{-1},\quad g\equiv 1+g_+g_-$$

Now T_l is determined by equating the individual wall free energies per site, $G(l)$ and $G(l+1)$, given in (4.5). To be specific, we adopt the form (4.2) for $\Sigma(T,\mu)$ and (4.13) for $W_2(l)$ with

$$w(T)=e^{-\Gamma}\approx\exp(-a\,\Delta\varepsilon/R_0k_BT)\ , \tag{A3}$$

as suggested by (3.8) and (3.9). The temperature dependence of Σ', U_2, and $\Delta\varepsilon$ may be regarded as negligibly weak compared with that displayed. One then has, as in (4.11),

$$\Sigma'(T_0-T_l)\equiv lW_2(T_l;l+1)-(l+1)W_2(T_l;l)\ , \tag{A4}$$

whence, as in (4.14),

$$\Delta T_l\approx 2T^{\dagger}l[w(T_0)]^{l-1} \tag{A5}$$

with $T^{\dagger}$ given by (4.15). This yields the estimate

$$\Delta_T W_2\approx\left|\left[\frac{dW_2}{dT}\right]_{T_l}\Delta T_l\right|$$

$$\approx 2W_2(T_l,\mu;l)\frac{aT^{\dagger}\Delta\varepsilon}{R_0k_B}\left[\frac{l}{T_l}\right]^2[w(T_0)]^{l-1}\ , \tag{A6}$$

whereas one has

$$\Delta_l W_2=W_2(T_l;l)[1-w(T_l)]\approx W_2(T_l;l)\ , \tag{A7}$$

and similarly for $\Delta_{l-1}W_2$. The presence of the extra small factor w^{l-1} in (A6) relative to (A7) ensures the validity of the desired condition (A2).

In similar fashion, one can also restore to the free energy the next largest term W_3, as in (5.1), and check that the resultant *shift* of the $[l]$:$[l+1]$ pseudoboundary is small relative to the phase widths ΔT_l or ΔT_{l+1}. Equating $\Delta\mathcal{F}_3([l])$ and $\Delta\mathcal{F}_3([l+1])$ from (5.1) gives, in place of (A4),

$$\Sigma'(T_0-T_l)=[lW_2(T_l;l+1)-(l+1)W_2(T_l;l)]$$

$$+[lW_3(T_l;l+1,l+1)-(l+1)W_3(T_l;l,l)]\ , \tag{A8}$$

where the third-order shift of the phase boundary is evidently represented by the second bracketed term. To embody the fundamental decay property (3.11) as in (4.13), we may adopt the form

$$W_3(T,\mu;l_1,l_2)=U_3w^{l_1+l_2}\ . \tag{A9}$$

Then the shift term in (A8) is of order $lw^{2l}(T_0)$, which is indeed small relative to the estimate (A5) for the phase widths ΔT_l or ΔT_{l+1} (by factors w^{l+1} and w^l, respectively).

*Present address: Department of Physics, University of Utah, Salt Lake City, UT 84112.

[1]S. Ostlund, Phys. Rev. B **24**, 398 (1981).

[2]D. A. Huse, Phys. Rev. B **24**, 5180 (1981).

[3]J. M. Yeomans and M. E. Fisher, J. Phys. C **14**, L835 (1981).

[4]J. M. Yeomans and M. E. Fisher, Physica **127A**, 1 (1984).

[5]M. E. Fisher and W. Selke, Phys. Rev. Lett. **44**, 1502 (1980).

[6]P. Bak and J. von Boehm, Phys. Rev. B **21**, 5297 (1980).

[7]J. Villain and M. B. Gordon, J. Phys. C **13**, 3117 (1980).

[8]M. E. Fisher and W. Selke, Philos. Trans. R. Soc. (London), Ser. A **302**, 1 (1981).

[9]A. M. Szpilka and M. E. Fisher, Phys. Rev. B (to be published).

[10]A. M. Szpilka and M. E. Fisher, Phys. Rev. Lett. **57**, 1044 (1986).

[11]P. Bak, Rep. Prog. Phys. **45**, 587 (1982).

[12]V. L. Pokrovsky and A. L. Talapov, *Theory of Incommensurate Crystals* (Harwood Academic, New York, 1984).

[13]R. Currat, in *Multicritical Phenomena*, edited by R. Pynn and A. Skjeltorp (Plenum, New York, 1984).

[14]J. D. Axe, Physica **120B**, 256 (1983).

[15]J. Rossat-Mignod, P. Burlet, H. Bartholin, O. Vogt, and R. Lagnier, J. Phys. C **13**, 6381 (1980). Note that the phase which we list, for simplicity, as $\langle 2\bar{3}\rangle$ is actually identified as $\langle 2\bar{3}\,2\bar{3}\,\bar{3}\rangle$.

[16]B. R. Cooper, in *Magnetism in Metals and Metallic Compounds*, edited by J. T. Łopuszański, A. Pękalski, and J. Przystawa (Plenum, New York, 1976).

[17]J. Smith and J. M. Yeomans, J. Phys. C **15**, L1053 (1982).

[18]D. de Fontaine and J. Kulik, Acta Metall. **33**, 145 (1985).

[19]R. Portier, D. Gratias, M. Guymont, and W. M. Stobbs, Acta Crystallogr. Sect. A **36**, 190 (1980).

[20]G. van Tendeloo and S. Amelinckx, Phys. Status Solidi A **43**,

553 (1977).
[21]A. Loiseau, G. van Tendeloo, R. Portier, and F. Ducastelle, J. Phys. (Paris) **46**, 595 (1985).
[22]Y. Komura and Y. Kitano, Acta Crystallogr. Sect. B **33**, 2496 (1977).
[23]D. de Fontaine, A. Finel, S. Takeda, and J. Kulik, in Noble Metal Alloys: *Phase Diagrams, Alloy Phase Stability and Thermodynamic Aspects,* edited by T. B. Massalski, W. B. Pearson, L. H. Bennett, and Y. A. Chang (Metallurgical Society, New York, 1986).
[24]R. Bruinsma and A. Zangwill, Phys. Rev. Lett. **55**, 214 (1985).
[25]J. D. Weeks, in *Phase Transformations in Solids,* edited by T. Tsakalakos (Elsevier, New York, 1984).
[26]J. M. Luck, S. Leibler, and B. Derrida, J. Phys. (Paris) **44**, 1135 (1983).
[27]M. Guymont, R. Portier, and D. Gratias, Acta Crystallogr. Sect. A **36**, 792 (1980).
[28]See, e.g., G. D. Price and J. Yeomans, Acta Crystallogr. Sect. B **40**, 448 (1984).
[29]J. Smith, J. Yeomans, and V. Heine, in *Modulated Structure Materials,* edited by T. Tsakalakos (Nijhoff, Boston, 1984).
[30]J. M. Yeomans and G. D. Price, Bull. Mineral. **109**, 3 (1986).
[31]F. Denoyer, A. H. Moudden, R. Currat, C. Vettier, A. Bellamy, and M. Lambert, Phys. Rev. B **25**, 1697 (1982).
[32]A. H. Moudden, D. E. Moncton, and J. D. Axe, Phys. Rev. Lett. **51**, 2390 (1983).
[33]D. Durand, F. Denoyer, R. Currat, and C. Vettier, Phys. Rev. B **30**, 1112 (1984).
[34]Y. Yamada and N. Hamaya, J. Phys. Soc. Jpn. **52**, 3466 (1983).
[35]R. Blinc, B. Ložar, F. Milia, and R. Kind, J. Phys. C **17**, 241 (1984).
[36]R. Blinc, P. Prelovšek, A. Levstik, and C. Filipič, Phys. Rev. B **29**, 1508 (1984).
[37]D. Durand, F. Denoyer, D. Lefur, R. Currat, and L. Bernard, J. Phys. (Paris) **44**, L207 (1983), point out that symmetry considerations for $NaNO_2$ should prevent an electric field stabilizing high-order C phases.
[38]M. S. Dresselhaus and G. Dresselhaus, Adv. Phys. **30**, 139 (1981).
[39]"Fractional" stage-(n/m) intercalates arise naturally in certain energy minimization models (Refs. 40 and 41) and neutron scattering evidence for a stage-$\frac{3}{2}$ phase in graphite-K has been presented by C. D. Fuerst, J. E. Fischer, J. D. Axe, J. B. Hastings, and D. B. McWhan, Phys. Rev. Lett. **50**, 357 (1983). The notation (n/m) implies a staging pattern with n graphite layers and m intercalate layers in each period.
[40]S. A. Safran, Phys. Rev. Lett. **44**, 937 (1980).
[41]S. Millman and G. Kirczenow, Phys. Rev. B **26**, 2310 (1982).
[42]M. J. Winokur and R. Clarke, Phys. Rev. Lett. **56**, 2072 (1986).
[43]F. C. Frank and J. H. van der Merwe, Proc. R. Soc. London **198**, 205 (1949); **198**, 216 (1949).
[44]P. Bak and V. J. Emery, Phys. Rev. Lett. **36**, 978 (1976).
[45]M. E. Fisher and D. S. Fisher, Phys. Rev. B **25**, 3192 (1982).
[46]See also T. Nattermann, J. Phys. (Paris) **43**, 631 (1982).
[47]M. E. Fisher, J. Stat. Phys. **34**, 667 (1984); in *Fundamental Problems in Statistical Mechanics VI,* edited by E. G. D. Cohen (North-Holland, Amsterdam, 1985), p. 1.
[48]M. E. Fisher, J. Chem. Soc., Faraday Trans. **2**, 1569 (1986) (Faraday Symp. 20).
[49]V. L. Pokrovsky and A. L. Talapov, Zh. Eksp. Teor. Fiz. **78**, 269 (1980) [Sov. Phys.—JETP **51**, 134 (1980)].
[50]S. N. Coppersmith, D. S. Fisher, B. I. Halperin, P. A. Lee, and W. F. Brinkman, Phys. Rev. Lett. **46**, 549 (1981); **46**, 869(E) (1981); Phys. Rev. B **25**, 349 (1982).
[51]J. Villain and P. Bak, J. Phys. (Paris) **42**, 657 (1981).
[52]V. L. Pokrovsky and A. Virosztek, J. Phys. C **16**, 4513 (1983).
[53]T. Nattermann, J. Phys. C **16**, 4113 (1983).
[54]J. Villain, J. Phys. (Paris) **43**, L551 (1982).
[55]S. Fishman and J. Yeomans, J. Phys. C **18**, 857 (1985); P. Bak, S. Coppersmith, T. Shapir, S. Fishman, and J. Yeomans, *ibid.* **18**, 3911 (1985).
[56]R. Lipowsky and M. E. Fisher, Phys. Rev. Lett. **56**, 472 (1986).
[57]The convex cover of $W_2(l)$ can be viewed as plotted by a taut string which is pulled upwards against the graph of W_2 vs l.
[58]Villian and Gordon (Ref. 7) in claiming to have established that a harmless staircase appears (in one domain of the ANNNI model phase diagram) overlook the significance of the higher-order interactions.
[59]See B. B. Mandelbrot, *The Fractal Geometry of Nature* (Freeman, San Francisco, 1983).
[60]We suppose here a "left-right" symmetry so that an $\alpha \mid \beta$ interface has the same tension as a $\beta \mid \alpha$ interface. Otherwise (4.27) represents the mean tension.
[61]P. Bak and R. Bruinsma, Phys. Rev. Lett. **49**, 249 (1982).
[62]S. Aubry, J. Phys. C **16**, 2497 (1983).
[63]In actuality there will be a cross-sectional *density* of interaction chains linking adjacent walls but we desire $W_2(l)$ which is, likewise, a cross-sectional density. The single-chain approximation may thus be viewed as an activity expansion valid, as stated, for small w^l.
[64]Ancillary support through NSF Grant No. DMR-81-17011.